EVALUATION OF BENT CAPS IN REINFORCED CONCRETE DECK GIRDER BRIDGES, PART 1

FINAL REPORT

RS 121

RESEARCH

EVALUATION OF BENT CAPS IN REINFORCED CONCRETE DECK GIRDER BRIDGES, PART 1

FINAL REPORT

RS 121

by

Christopher Higgins, degree (ex. Ph.D.), title (ex. Associate Professor)
Ahmet Ekin Senturk, title (ex. Associate Professor)

and

Carl C. Koester, title (ex. Associate Professor)

School of Civil and Construction Engineering
Oregon State University
Corvallis, OR 97331

for

September 2008

Technical Report Documentation Page

1. Report No. OR-RD-07	2. Government Accession No.	3. Recipient's Catalog No.
4. Title and Subtitle Evaluation of Bent Caps in Reinforced Concrete Deck Girder Bridges, Part 1		5. Report Date September 2008
		6. Performing Organization Code
7. Author(s) Christopher Higgins, Ahmet Ekin Senturk and Carl C. Koester		8. Performing Organization Report No.
9. Performing Organization Name and Address School of Civil and Construction Engineering Oregon State University Corvallis, OR 97331		10. Work Unit No. (TRAIS)
		11. Contract or Grant No. RS 121
12. Sponsoring Agency Name and Address Oregon Department of Transportation Research Unit 200 Hawthorne Ave. SE, Suite B-240 Salem, OR 97301-5192		13. Type of Report and Period Covered Final Report
		14. Sponsoring Agency Code
15. Supplementary Notes		

16. Abstract
This report describes research conducted to enable evaluation of existing vintage bent cap beams in reinforced concrete deck girder bridges. The report is organized into two parts: 1) flexural anchorage capacity response and prediction of reduced development length due to beneficial column axial compression and 2) structural performance of bent cap systems and their analytical evaluation. Each of these parts including descriptions of the experimental specimens and results of analytical studies is described separately. The research results from both studies are combined and used in an example to demonstrate the rating of an actual 1950's vintage RCDG bent cap beam for continuous and single trip permit loads.

17. Key Words Bent caps, anchorage, structural performance, bridge.	18. Distribution Statement Copies available from NTIS, and online at http://www.oregon.gov/ODOT/TD/TP_RES/

19. Security Classification (of this report) Unclassified	20. Security Classification (of this page) Unclassified	21. No. of Pages 70	22. Price

Technical Report Form DOT F 1700.7 (8-72) Reproduction of completed page authorized Printed on recycled paper

i

SI* (MODERN METRIC) CONVERSION FACTORS

APPROXIMATE CONVERSIONS TO SI UNITS

Symbol	When You Know	Multiply By	To Find	Symbol
		LENGTH		
in	inches	25.4	millimeters	mm
ft	feet	0.305	meters	m
yd	yards	0.914	meters	m
mi	miles	1.61	kilometers	km
		AREA		
in^2	square inches	645.2	millimeters squared	mm^2
ft^2	square feet	0.093	meters squared	m^2
yd^2	square yards	0.836	meters squared	m^2
ac	acres	0.405	hectares	ha
mi^2	square miles	2.59	kilometers squared	km^2
		VOLUME		
fl oz	fluid ounces	29.57	milliliters	ml
gal	gallons	3.785	liters	L
ft^3	cubic feet	0.028	meters cubed	m^3
yd^3	cubic yards	0.765	meters cubed	m^3
	NOTE: Volumes greater than 1000 L shall be shown in m^3.			
		MASS		
oz	ounces	28.35	grams	g
lb	pounds	0.454	kilograms	kg
T	short tons (2000 lb)	0.907	megagrams	Mg
		TEMPERATURE (exact)		
°F	Fahrenheit	(F-32)/1.8	Celsius	°C

APPROXIMATE CONVERSIONS FROM SI UNITS

Symbol	When You Know	Multiply By	To Find	Symbol
		LENGTH		
mm	millimeters	0.039	inches	in
m	meters	3.28	feet	ft
m	meters	1.09	yards	yd
km	kilometers	0.621	miles	mi
		AREA		
mm^2	millimeters squared	0.0016	square inches	in^2
m^2	meters squared	10.764	square feet	ft^2
m^2	meters squared	1.196	square yards	yd^2
ha	hectares	2.47	acres	ac
km^2	kilometers squared	0.386	square miles	mi^2
		VOLUME		
ml	milliliters	0.034	fluid ounces	fl oz
L	liters	0.264	gallons	gal
m^3	meters cubed	35.315	cubic feet	ft^3
m^3	meters cubed	1.308	cubic yards	yd^3
		MASS		
g	grams	0.035	ounces	oz
kg	kilograms	2.205	pounds	lb
Mg	megagrams	1.102	short tons (2000 lb)	T
		TEMPERATURE (exact)		
°C	Celsius	1.8C+32	Fahrenheit	°F

*SI is the symbol for the International System of Measurement

ii

ACKNOWLEDGEMENTS

DISCLAIMER

TABLE OF CONTENTS

APPENDICES

APPENDIX A

TABLE OF TABLES

TABLE OF FIGURES

1.0   INTRODUCTION

Many conventionally reinforced concrete deck girder (RCDG) bridges were built in the US during the 1950s throughout the expansion of the Interstate System. Designs followed the AASHO standard of the time, which permitted higher shear stress in concrete and reduced detailing requirements than permitted by current specifications. Many of these bridges exhibit diagonal cracking of the main girders and bent caps that has been attributed to vintage design, increased traffic volume, higher truck load magnitudes, and temperature and shrinking effects. While these RCDG bridges are nearing the end of their design lives, wholesale replacements or renewals are not possible due to the large numbers of bridges.

This report describes research conducted to enable evaluation of existing vintage bent cap beams in reinforced concrete deck girder bridges. The report is organized into two parts: 1) flexural anchorage capacity response and prediction of reduced development length due to beneficial column axial compression and 2) structural performance of bent cap systems and their analytical evaluation. Each of these parts including descriptions of the experimental specimens and results of analytical studies is described separately. The research results from both studies are combined and used in an example to demonstrate the rating of an actual 1950's vintage RCDG bent cap beam for continuous and single trip permit loads.

Part 1 of the report details experimental results from sub-assemblage tests of 1950's vintage reinforced bent cap column anchorages and compares these with capacity prediction models. A series of specimens was constructed to represent 1950's vintage flexural bar anchorages terminating in reinforced concrete column sections. The test arrangement allowed the flexural bars to be loaded while axial compressive load was independently applied to the column section. The experimental data were compared to recent development length equations for straight bar anchorages from AASHTO 2005 and ACI 2005. The service level dead load axial force magnitude applied to the column increased the anchorage capacity of the specimens by 60% on average. Further increasing the axial force to the 1957 AASHO specified maximum allowable column stress did not significantly increase the anchorage capacity. Current US building and bridge design specifications underestimated the available anchorage strength for specimens with axial compression.

The addition of active confinement effects enabled better prediction of anchorage capacity for the specimens and may provide a better estimate of capacity for vintage 1950's RCDG flexural bar anchorages terminating in column sections. A development length modification factor (κ) was introduced to include the beneficial effects of column axial compression stress. Upper and lower limits on κ, were established to restrict the benefit of high column compression stress due to limitations seen in previous research and neglect the contribution of low column axial compression stresses.

Part 2 of the report describes the laboratory assessment of six realistic full-scale replicas of in-service bent caps with 1950s vintage details including the overall geometry, reinforcement configuration, and material properties. The test specimens were a subassemblage of the pertinent bridge components at the bent cap region including the integral columns, cap beam, and portions of the monolithic internal girders that frame into the cap. Test variables included shear span-to-depth (a/d) ratio, number of flexural bars anchored in the columns, flexural reinforcement cut-off locations, web reinforcement size and grade, and loading type (static and fatigue loading). The bent caps were loaded indirectly similar to their in-field counterparts via portions of the integral girders. The specimens were loaded to failure using an incremental cyclic load protocol. To simulate the effect of 50 years of ambient traffic loading, 1,000,000 cycles of fatigue loading based on a unique load protocol derived from in-situ measured stress ranges from three in-service bridges was applied to one of the specimens prior to failure testing.

Various analytical methods were applied to the laboratory specimens for capacity prediction including ACI 318 shear design methods, the Modified Compression Field Theory (MCFT) sectional analysis approach, strut-and-tie models, mechanical models, and non-linear finite element analysis.

The embedded reinforcement at the anchorage zone, the web reinforcement, and the a/d ratio were all found to be pertinent parameters which affect the strength of bent cap specimens. High cycle fatigue did not cause a significant degradation in the ultimate capacity for a specimen with light web reinforcement although debonding of the stirrups was observed at the characteristic diagonal crack vicinity. Best results for capacity prediction were achieved with non-linear finite element analysis and with The Modified Zararis Mechanical Model. A spreadsheet application was developed to conduct the Modified Zararis Mechanical Model. Further finite element analyses showed that the strength of specimens with heavy web reinforcement may be more sensitive to the effects of bond fatigue.

2.0   TESTING AND EVALUATION OF BENT CAP FLEXURAL REBAR

Reinforced concrete deck-girder (RCDG) bridges are a mainstay of the U.S. bridge population. Many of these are reaching the end of their originally intended design life and are showing signs of deterioration. Resources are not available for wholesale replacements and therefore many of these bridges must remain in service. Agencies responsible for operation of these bridges must continue to inspect and evaluate their fitness for purpose.

RCDG bridges were widely used through the early 1960's and comprise a large proportion of the US bridge inventory. RCDG bridges constructed prior to adoption of ASTM A305-50, which standardized reinforcing bars, are generally well detailed: containing hooks and bends for anchorage of flexural reinforcing bars. ASTM A305-50, however, relaxed the anchorage and bond requirements and thus, RCDG's designed during the 1950's and early 1960's commonly contain poor flexural detailing. Significant research has already been conducted to better understand vintage RCDG bridge girder performance (*Higgins et. al., 2004*) and additional research has recently been completed to assess transverse bent caps for these bridges. The bent caps are a major component of the bridge superstructure, and are considered a non-redundant component, which in the event of member failure may result in collapse of the bridge. Due to poorly detailed anchorages, large numbers of 1950's vintage RCDG bridge bent caps are commonly rated as inadequate using conventional analysis methods. Overly conservative bridge ratings can adversely affect major transportation routes with unnecessary weight limits, restrictions, and needless replacement or strengthening. To provide better tools to predict the strength and behavior of bent cap anchorages, research was undertaken. This report details experimental results from sub-assemblage tests of 1950's vintage reinforced bent cap column anchorages and compares these with capacity prediction models.

2.1   BACKGROUND

Reinforced concrete specifications have continued to evolve in the treatment of anchorage and bond of reinforcing bars. In the early part of the 20th century, reinforcing bars were often proprietary and a variety of different bar shapes were employed, including: square, twisted square, plain round and deformed bars. Due to the variability in bar types, hooks and bends were required to ensure proper anchorage and bond. Early work by Clark (*1946*) evaluated 17 commercially available bars and examined the effects of the geometric properties on bond. Based on this research and subsequent studies (*Clark 1949*) reinforcing bar standards were developed, which became the modern deformed bars seen in ASTM A305-49 and eventually the contemporary ASTM-A615 specifications (*Ferguson et al., 1965*).

Upon the implementation of ASTM A305-50, reinforced concrete design practice for bond and anchorage changed rapidly from that of the earlier decades. Detailing requirements and

allowable stresses were changing quickly and according to ACI 208-58: "Acceptance by the ACI Building Code committee of the ASTM A305 definition of a deformed bar produced an immediate drastic change in both structural and general practice, resulting in the almost immediate disappearance of old-style nonconforming deformed reinforcement." Additionally, review of U.S. codes prior to the 1950's shows that allowable bond stress for straight bar anchorages was lower after the acceptance and implementation of ASTM A305-50, as seen in Table 1.

Table 2.1: Comparison of bond equations used in design

Code Specifications	Allowable Shear Stress In Concrete (psi)				Allowable Bond Stress (psi) (Straight) or **Dev. Length (in)**	Allowable Bond Stress (psi) (Hooked) or **Dev. Length (in)**
	With Web Reinforcement		Without Web Reinforcement		Structural or Inter. Gr.	Structural or Intermediate Grade
	Long. Bars not anchored	Long. Bars anchored	Long. Bars not anchored	Long. Bars anchored	(Not Anchored)	(Anchored By Hooks or Such)
AASHO 1944	$0.046f'_c$	$0.06f'_c$	$0.02f'_c$	$0.03f'_c$	$0.033f'_{c\ (max\ 100)}$	$0.05f'_{c\ (max\ 150)}$
AASHO 1949	$0.046f'_c$	$0.06f'_c$	$0.02f'_c$	$0.03f'_c$	$0.05f'_{c\ (max\ 150)}$	$0.075f'_{c\ (max\ 225)}$
AASHO 1953	$0.075f'_c$	$0.075f'_c$	$0.02f'_c$	$0.03f'_c$	$0.10f'_{c\ (max\ 350)}$	$0.10f'_{c\ (max\ 350)}$
AASHO 1957	$0.075f'_cbjd$	$0.075f'_cbjd$	$0.02f'_{c\ (max\ 75)}$	$0.03f'_{c\ (max\ 90)}$	$0.10f'_{c\ (max\ 350\ )}$	$0.10f'_{c\ (max\ 350)}$
AASHO 1961	$0.075f'_cbjd$	$0.075f'_cbjd$	$0.02f'_{c\ (max\ 75)}$	$0.03f'_{c\ (max\ 90)}$	$0.10f'_{c\ (max\ 350)}$	$0.10f'_{c\ (max\ 350)}$
AASHO 1969	$0.075f'_cbjd$	$0.075f'_cbjd$	$0.02f'_{c\ (max\ 75)}$	$0.03f'_{c\ (max\ 90)}$	$0.10f'_{c\ (max\ 350)}$	$0.10f'_{c\ (max\ 350)}$
AASHO 1973(ASD)	$0.075f'_cbjd$	$0.075f'_cbjd$	$0.02f'_{c\ (max\ 75)}$	$0.03f'_{c\ (max\ 90)}$	$\dfrac{4.8\sqrt{f'_c}}{D}\ _{(max\ 500)}$	$\dfrac{4.8\sqrt{f'_c}}{D}\ _{(max\ 500)}$
AASHO 1973(USD Development Length)	-	$4\varphi\sqrt{f'_c}$	-	$6\varphi\sqrt{f'_c}$	$\dfrac{0.04A_sf_y}{\sqrt{f'_c}}$ **(in)**	$f_h = k*\sqrt{f'_c}\ \dfrac{0.04A_sf_h}{\sqrt{f'_c}}$ **(in)**
ACI 1941	$0.06f'_c$	$0.12f'_c$	$0.02f'_c$	$0.03f'_c$	$0.05f'_{c\ (max\ 200)}$	$0.056f'_{c\ (\ max\ 200)}$
ACI 1947	$0.06f'_c$	$0.12f'_c$	$0.02f'_c$	$0.03f'_c$	$0.05f'_{c\ (max\ 200)}$	$0.075f'_{c\ (max\ 250)}$
ACI 1951	-	$0.12f'_c$	-	$0.03f'_c$	$0.10f'_{c\ (max\ 350)}$	$0.10f'_{c\ (max\ 350)}$
ACI 1956	-	$0.12f'_c$	-	$0.03f'_c$	$0.10f'_{c\ (max\ 350)}$	$0.10f'_{c\ (max\ 350)}$
ACI 1963(ASD)	-	$1.1\sqrt{f'_c}$	-	$1.1\sqrt{f'_c}$	$\dfrac{4.8\sqrt{f'_c}}{D}\ _{(max\ 500)}$	$\dfrac{4.8\sqrt{f'_c}}{D}\ _{(max\ 500)}$
ACI 1963(USD)	-	$10\varphi\sqrt{f'_c}$	-	$\phi(1.9\sqrt{f'_c}+2500\dfrac{p_wVd}{M})$	$\dfrac{9.5\sqrt{f'_c}}{D}\ _{(max\ 800)}$	$\dfrac{9.5\sqrt{f'_c}}{D}\ _{(max\ 800)}$
ACI 1971 (USD Development Length)	-	-	-	-	$\dfrac{0.04A_sf_y}{\sqrt{f'_c}}$	$f_h = k*\sqrt{f'_c}\ \dfrac{0.04A_sf_h}{\sqrt{f'_c}}$ **(in)**

In the AASHO Standard Specifications 1949 to 1953, the allowable bond stress increased from 150 psi to 350 psi for straight bar anchorages. This confidence in the new reinforcing bars can also be seen in publications of the time such as ACI 208-1950. Due to the higher allowable bond stress apparently available with the standardized bars, hooks and bends were then considered unnecessary. A lower stress value for straight bar anchorages was also eliminated from the codes of this period. During this early period of adoption, many of the constructed bridges and other structures have what are now considered deficient flexural reinforcing steel anchorages that terminate in the supporting columns. Of particular concern are bent cap members containing flexural straight bar anchorages with relatively short embedment's. Often, a large percentage of the flexural reinforcing bars used to develop the needed bent cap strength are terminated prior to the column section, resulting in an apparent member strength deficiency.

Experimental research was undertaken to examine typical anchorage conditions that would be present in many 1950's vintage bridges. The application of this work is to better estimate anchorage capacity of flexural bars terminating in the supporting columns for existing RCDG bridges with significant diagonal cracks at the bent cap and column interface (Figure 2.1 and Figure 2.2). Research conducted at Oregon State University on 1950's vintage RCDG bridge bent caps also shows diagonal cracks forming at the interface of the column and bent (Figure 2.2). These diagonal cracks at the column-bent cap connection place additional demand on the flexural reinforcing bar anchorage and the ability to develop the necessary bar resistance is uncertain (Figure 2.1).

Figure 2.1: Typical diagonal crack forming at column bent connection (diagonal crack highlighted)
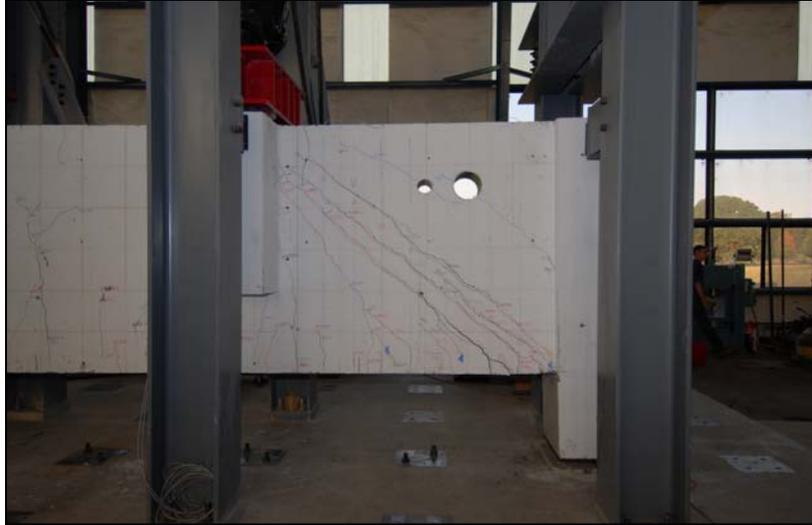
Figure 2.2: Typical diagonal crack forming at column bent connection roller side reaction

2.2 BOND, ANCHORAGE, AND DEVELOPMENT LENGTH

Bond is the means by which force is transferred between the concrete and reinforcing steel (*MacGregor and Wright 2005*). It is dependent on the reinforcing bar size, geometric and structural configurations, and concrete properties (*ACI 408R-03, 2004*). Average bond stress, μ, can be calculated (*Peabody 1946; Large 1957; Ferguson 1979; ACI 408R-03 2004: MacGregor and Wright 2005*) as:

$$\mu = \frac{V}{\sum_o *jd}$$
(2.1)

where, V is shear force at the section, Σ_o is the total sum of the perimeter of flexural reinforcing bars at the section of interest, and jd is the internal lever arm for the elastic section. The actual bond stress (*MacGregor and Wright 2005*) may be calculated as:

$$\mu = \frac{df_s d_b}{4d_x}$$
(2.2)

Here, df_s is the change in rebar stress over length d_x, and d_b is the diameter of the bar. Anchorage and development of rebar stress are related in that reinforcing bars must have adequate anchorage (sufficient embedded length) to develop the required bar stress rather than pullout from the concrete prematurely. In vintage RCDG bridges, after formation of diagonal cracks, additional demand is produced on the flexural bars and because of poor detailing, the bars commonly do not have sufficient anchorage, or embedded length, to ensure yielding of the bars. The 17th edition of AASHTO and AASHTO-LRFD (*2005*) specifications require over 45 in. (1143 mm) of embedment for a #11 (36) Gr. 40 rebar. Review of a large number vintage RCDG's plans revealed that many column anchorages only provide a fraction of this embedment length. Darwin (*2005*) reviewed the AASHTO, ACI 318-05, ACI 408, CEB-FIP Model Code

6

1990, and Eurocode 2, and showed that AASHTO provided the lowest factor of safety for development length, indicating that other specifications would require even longer embedment's.

2.2.1 LITERATURE REVIEW

Much research has been completed in the area of bond, development length, splice length and anchorage with the earliest work done in 1877 by Hyatt (*ACI 408R-03, 2004*). A large portion of bond research has been done using beam specimens, but several different specimen configurations and testing apparatuses have been developed. These include traditional pullout tests, beam end specimens or cantilever beam specimens, eccentric beam specimens, tension tests, bond beams, modified bond beam, and many other variations (*ACI 408, 1966; Ferguson, 1979; ACI 408R-03, 2004; Chapman, 1987*).

Considerable research has been done using pullout tests, in which the specimens are usually relatively small (*Clark, 1946; Clark, 1949; Mains, 1951; Ferguson, 1954 Untrauer and Henry, 1965; Goto, 1971; Robins and Standish, 1982; Cairns and Jones, 1982; Gambarova and Karakoc1982; Soroushian and Choi, 1986; Ezeldin and Balaguru, 1989; Malvar, 1992; Mo and Chan, 1995; Baldwin and Clark, 1995; Carins and Jones, 1995; Schroder and Wood, 1996*) and these tests are still widely used. Pullout tests range from small cubes to large rectangular blocks. End beam specimens have also been used (*Lutz, 1970; Morita and Fujii, 1982; Darwin and Graham, 1993*), as well as conventional beam specimens (*Clark, 1949; Mains, 1950; Ferguson et al., 1965*). Beam tests continue to be used by many researchers (*Harajli et al., 2004; Jeppsson and Thelandersson, 2003*).

The primary focus of this investigation is performance of straight bar anchorages of bent cap flexural bars terminating in columns, which can have significant axial confinement (active pressure acting across the splitting plane). While a large body of work exists on bond, anchorage, and development length in rebar anchorages in flexural tension zones (in beams), as well as from reversed cyclic loading tests, these are not applicable to the present research. Further, hooked anchorages, which have also been studied in great detail, are not included here as they too do not apply to the present work.

Significant background on bond and anchorage is available in the ACI 408 committee report "Bond Stress State of the Art" (*2004*). Earlier versions were released in 1979 and 1966. The "State of the Art" report details bond analysis models and the factors influencing bond. These parameters include: the concrete strength, the amount of concrete surrounding the bar (cover), transverse reinforcement, rebar geometries and strength, and rebar surface conditions. Previous research on anchorage at beam-column interfaces has shown anchorage, short embedment lengths, transverse steel, and lateral pressure on the specimen are influential parameters and this related research is described subsequently.

One of the earliest studies was by Untrauer and Henry (*1965*) in which 37 pullout specimens were tested, 28 specimens tested with normal confining force. The small specimens were 6 x 6 x 6 in. (154 x 154 x 154 mm) cubes of concrete, with single bars of size #6(19) and #9(29). The normal confining pressure varied from 237 to 2370 psi (1.6 to 16.3 MPa), and higher confining

pressure was seen to increase the ultimate bond strength by the square root of the normal pressure.

Doerr (*1978*) studied small cylindrical specimens in an effort to quantify strains in the reinforcing and concrete, and tested 25 specimens. The specimens were 6 x 24 in. (150 x 600 mm) cylinders with two strain gauges embedded near the reinforcing bar; a notch was placed at the center to ensure crack propagation at the middle of the specimen. Specimens contained a single #5 (16) reinforcing bar. The lateral pressure applied to the specimens was 0, 725, 1450, and 2175 psi (0, 5, 10, and 15 MPa). Average compressive strength of the concrete was 5200 psi (35.9 MPa). The embedment length was 20 in. (500 mm) and strains were measured by notches in the reinforcing bar.

Gambrova and Karakoc (*1982*) investigated average bond stress, confinement stress, bar slip, and crack width. The test specimens were square with triangular portions removed from the top and bottom of the specimen. A total of 7 specimens were tested, with three relevant to the current work. Specimens were 12 x 2 in. (300 x 50 mm), with 6 in. (150 mm) of concrete in the center sloping to the removed tops. Reinforcing was a single #6 (18 mm) bar, without transverse steel. Tests were run with variable confinement pressure, an embedment of 5 ribs (2.12 in., 54 mm) and a constant crack width for each test. It was found that in the early stages of testing, the confining pressure was not utilized until 20% of the maximum pullout load, and that in the final stages of the test, a residual strength was present due to crushed concrete in front of the ribs, and that the crack width for the values tested did not affect maximum bond.

Robins and Standish (*1982*) examined the affects of lateral pressure on both cubes and semi-beams. The cubes were 4 x 4 x 4 in. (100 x 100 x 100 mm) and the semi-beam specimens were 4 x 6 x 12 in. (100 x 150 x 300 mm). A total of 151 specimens with light-weight concrete was tested with 72 cubes, 79 semi-beams, and 8 normal-weight concrete semi-beams. Lateral pressure was applied up to 4000 psi (28 MPa). Average concrete strength was 4350 psi (30 MPa). Small plain and deformed round bars of 0.32 and 0.47 in. (8 and 12 mm) diameter were used in the study. It was found that the cube tests tended to overestimate bond capacity as compared with semi-beam specimens. It was also found that the lateral pressure increased the measured bond strength by 110%. Two modes of failure were determined with the deformed bars: a splitting or bursting failure and a shearing failure which was observed at higher lateral pressure.

Research by Eligehausen, *et al*. (*1983*) tested 125 beam-column connections. The majority of specimens were tested under reversed cyclic loading. However, 42 were tested under monotonic loading and for varying parameters. The specimen size was dictated by bar diameter, total column width was $15d_b$, thickness was $7d_b$ and the height was 12 in. (304 mm). Reinforcing bars of #6 (19), #8 (25), and #10 (32) size were tested in the series, and the specimens were highly confined with a stirrup spacing of 3.3 in. (83 mm) on-center. The embedment length was $5d_b$ and a total of seven series of tests was performed, with series #6 being most relevant to the current work. For this series, the transverse column pressure varied from 725 to 1914 psi (5 to 13.1 MPa). The bond behavior was determined to be improved by adding transverse pressure, and the maximum observed benefit was a 25% increase in strength.

Robins and Standish (*1984*) in an extension of their previous research to light-weight concrete specimens looked at specimens with applied lateral loads from 0 to $0.3f_c$. They found that increasing the lateral pressure above $0.3f_c$ did not increase the ultimate pullout load. A limiting value of $1.8\sqrt{f_c}$ for ultimate bond was found for the light-weight concrete investigated.

Navaratnarjah and Speare (*1986*) using three different bar types (Torbar, Hybar, and Twisted Square) and tested a number of specimens. The specimens were 20 x 20 x 15 in. (500 x 500 x 375 mm), with a pair of #8 (25) bars tested each time. The column type section had a tie spacing of 1.5 in. (40 mm). Cover varied from 1 to 4 d_b, while lateral pressure varied from 0 to $1/3f_c$ and the concrete strength on average was 5075 psi (35 MPa). Bar casting location was observed to affect the capacity from 30 to 50%. Bond stress was found to increase for covers up to 3.5 d_b, and with lateral pressure in proportion to $\sqrt{f_c}$, and was limited by $0.25f_c$.

Malavr (*1992*) investigated the affects of confining pressure on deformed reinforcement for 12 specimens. Specimens were small 3 in. (76 mm) diameter by 4 in. (100 mm) long specimens with #6 (19) reinforcing bars. It was found that confining pressure increased bond strength.

Nagatomo and Kaku (*1992*) performed a study of bond under both lateral pressure and tension, a total of 46 specimens 16 x 16 x 6 in. (400 x 400 x 155 mm) was tested with single #7 (22) reinforcing bars. It was found that lateral pressure increased bond strength linearly up to a point, after which the benefits was found to level off at 30% of compression strength. This beneficial effect was found to be not as effective with cover above 2.5 d_b.

In a study of deep light-weight concrete beams by Kong *et al.* (*1996*), it was determined that the tensile reinforcement development could be reduced to $10d_b$ without adversely affecting strength but this was with high bearing pressure at the bearings. The bearing area used for the specimens was 4 x 3.5 x 1.13 in (100 x 89 x 30 mm).

Baldwin and Clark (*1995*) examined 96 single reinforcing bar specimens with 0.31 in. (8 mm) diameter and inadequate anchorage. Both cover and anchorage length were varied with cover varying between one and six d_b. Anchorage length varied from 30 to 2.5 d_b. This study indicated that ultimate load tended toward a linear function of anchorage length, and bar anchorage less than three d_b could be disregarded.

Gambarova and Rosati (*1996*) conducted follow-up work using the same specimen types described previously. They investigated 16 specimens with large and small diameter reinforcing bars under varying transverse pressure, and 4 specimens with a constant transverse pressure were investigated. Research confirmed that ultimate pullout load for specimens with constant confining pressure was linear and bond was generally not sensitive to the kinematic path especially at higher confining stresses.

Walker *et al.* (*1997*) investigated 23 specimens of size 24 x 11 in. (607 x 280 mm) with varying depth between 10 to 15 bar diameters. Each specimen had two top bars and two bottom bars. The reinforcing bars used in the study were #3, #4, and #5 (8, 12, and 16 mm). Variables examined included bar diameter, cover, lateral pressure, concrete strength, as well as horizontal and vertical bar spacing. Results indicated that top cast bars exhibit less capacity than bottom bars.

Orientation of casting seems insensitive for bars in pairs, and bond increased with cover and concrete strength. Walker *et al*. (*1999*) used results from earlier research to compare them with European codes. The ultimate bond prediction was a function of the concrete strength, cover, bar diameter, and lateral pressure.

Engstrom, *et al.,* (*1998*), examined the affects of anchorage length, varying confinements due to stirrup configurations and concrete compressive strength. The specimens were approximately 15.5 in. (400 mm) concrete cubes with one or two embedded deformed bars. The longest anchorage length investigated was 19.6 in. (500 mm). A total of 30 specimens was tested with #5 (16) bars. Results showed that stirrup confinement increased the anchorage capacity of the specimen.

Overall, previous research on transverse pressure to longitudinal reinforcement has been conducted on relatively small sized specimens with single or two bar groups. Also, the concrete strength for most specimens is much higher than that specified for bridges in the 1950's and that used in the present research. Realistic large-size column sections and large diameter reinforcing bars and bar groups, with confining pressures are not available in the literature, and thus research was conducted on realistic, large-sized bridge beam-column anchorages as described subsequently.

2.3   EXPERIMENTAL PROGRAM

2.3.1 Test Specimens

A series of specimens was constructed to represent 1950's vintage flexural bar anchorages terminating in reinforced concrete column sections. The column geometry investigated was 24 x 24 x 72 in. (610 x 610 x 1829 mm). A total of twelve specimens were constructed from July to November 2006, and test variables included anchorage length, number of anchorage bars, transverse column reinforcement, and column axial pressure as illustrated in Figure 2.3.
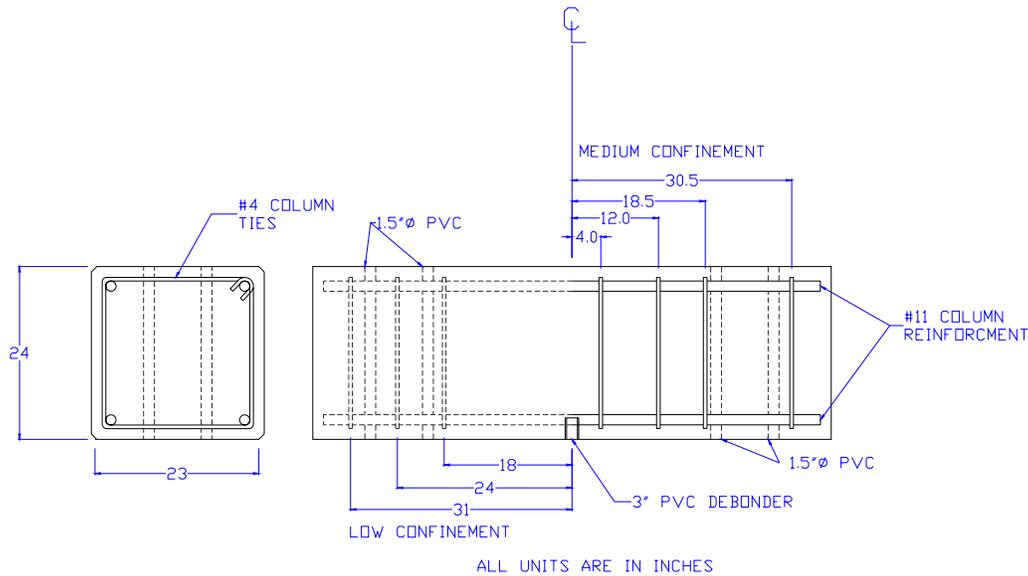
Figure 2.3: Typical column reinforcing details for all specimens, both low and medium stirrups

Anchorage bars were placed perpendicular to the main column cross section of the specimen during casting. Due to the positioning of the bars, they are not considered top bars. This is consistent with in-situ details where, due to construction staging and cast sequencing, less than 12 in. (305 mm) of fresh concrete is placed below the bars. The naming convention used for the specimens was based on the number of bars, transverse reinforcing, axial load in the column, and anchorage embedment length. The specimen naming convention is illustrated in Figure 2.4. The number of bars varied from 1 to 4. The transverse reinforcement was described either as medium or low with #4 (13) nominal Grade 40 (275 MPa) ties either spaced at 8 in. (203 mm) or not included in the anchorage zone (Figures 2.3, 2.5, 2.6 and 2.7). Three axial loads were used during the tests: 0, 200 kips (890 kN), and 500 kips (2224 kN), and each of these was abbreviated as 0, 2, or 5. The embedment lengths of the anchorage bars were 8, 12 or 21 in. (203, 305, 533 mm).
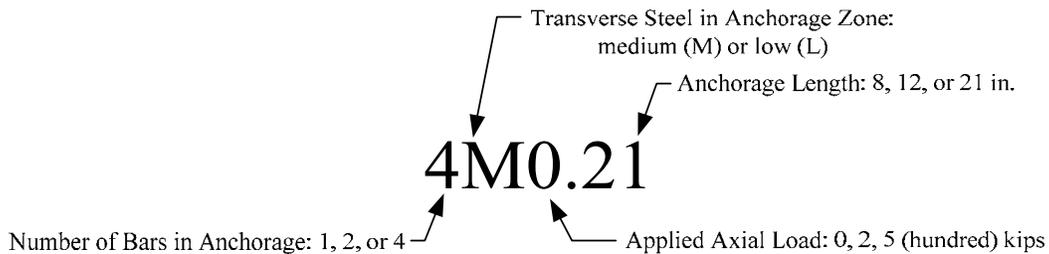
Figure 2.4: Specimen designation schematic

The steel reinforcing used predominantly in the members of interest for this study are ASTM A305-50 (*1950*) intermediate Grade bars (nominal Gr.40 (279 MPa)). These bars have a lower yield value than the rebar available for this research because modern #11 (36) deformed bars are commonly only available in Grade 60 (420 MPa). The size, spacing and details of the column anchorage was based on a review of the database of bridges in Oregon (*Higgins et al., 2002*) and was performed in conjunction with full-sized bent cap testing conducted at Oregon State University. The rebar spacing in the column sub-assemblage specimen was slightly larger than that used in the full-size bent cap column specimens due to spacing and constructability constraints. The anchorage spacing for the bars in the column section was 4 in. (102 mm) on-center, while bars in the full-size bent caps were 3.5 in. (89 mm) on-center.

2.3.2 Material Properties

Concrete was provided by a local ready-mix supplier for all specimens. The concrete mix design was based on 1950's AASHO "Class A" concrete used in previous research at OSU (*Higgins et al., 2003*). Specified compressive strength was 3000 psi (21 MPa), that is comparable to the specified design strength in the original 1950's bridges. Actual concrete compressive strengths were determined from 6 x 12 in. (152 x 305 mm) cylinders which were tested for 28 day and day-of-test strengths in accordance with ASTM C39M/C 39M-05 and ASTM C617-05. Day-of-test compressive strengths are shown in Table 2.2.

Table 2.2: Concrete compressive strength at day of test

Series	Specimen	Test f'$_c$ psi	Test f'c (MPa)
1	1M021	3790	(26)
	1M08	4150	(28)
	1M012	4360	(30)
2	2L021	3550	(24)
	2M021	3550	(24)
	4L021	3790	(26)
	4M021	3790	(26)
3	4L221	3070	(21)
	4M221	2960	(20)
	4L521	3240	(22)
	4M521	3080	(21)

The aggregate composition for the mix was reported by the supplier to be: 97% passing the 3/4 in. sieve (19 mm), 82% passing 5/8 in. (16 mm), 57% passing 1/2 in. (12.5 mm), 33% passing 3/8 in. (9.5 mm), 21% passing 5/16 in. (8 mm), 9.3% passing 1/4 in. (6.3 mm), 3.0% passing #4 (4.75 mm), 0.6% passing #8 (2.36 mm) and 0.3% passing the #200 (0.075 mm) sieve. The sand composition of the mix was also reported as: 99.7% passing the 1/4 in. sieve (6.3 mm), 96.8% passing #8 (2.36 mm), 59.4% passing #16 (1.18 mm), 44.9% passing #30 (0.600 mm), 17.9%

passing #50 (0.300 mm), 3.7% passing #100 (0.150 mm) and 1.7% passing the #200 (0.075 mm) sieve. The coarse aggregate was from Willamette River bed deposits and was smooth rounded basaltic rock.

2.3.3 Transverse and Flexural Reinforcing

Reinforcing cages for the columns consisted of both transverse and flexural reinforcing bars. All transverse reinforcing was ASTM 615 nominal Gr. 40 (276 MPA), which corresponds to Intermediate Grade (40 ksi, 276 MPa) A305 steel used in the 1950's. The tie spacing in the column section varied for different specimens as seen in Figure 2.3, Figure 2.5 and Figure 2.6. The steel mechanical properties were determined in accordance with ASTM E8-04a (*2005*), and the yield stress for the ties was 54 ksi (374 MPa) as shown in Table 2.3.

Figure 2.5: Typical medium confinement column cage prior to casting

Figure 2.6: Typical low confinement column cage prior to casting (no ties located in the anchorage zone)

Column bars (flexural reinforcing) for the specimens were taken from two different heats of ASTM 615/615M-05a (*2005*) Gr. 60 #11(36) bars. Series 1 was taken from one heat while series 2 and 3 were from another heat. These bars were tested according to ASTM E8-04a (*2005*) machined to the 505 specimen size. The yield stress for Series 1 column bars was 71 ksi (490 MPa) and the yield stress for series 2 and 3 was 66 ksi (454 MPa), as seen in Table 3. The column bars were sheared into 69 in. (1753 mm) lengths providing 1.5 in. (38 mm) of clear cover at the specimen ends.

2.3.4 Anchorage Bars

The anchorage bars used for specimens were standard ASTM A615/615M-05a (*2005*) Grade 60 #11 (36) bars taken from a single heat of steel. The bars were tested according to ASTM E8-04 (*2005*). The yield stress was 66 ksi (1674 MPa) and ultimate strength was 114 ksi (786 MPa). The bars were all provided in 70 in. (1778 mm) lengths by a rebar fabricator. When the bars were placed into the specimens prior to casting, the mill markings were purposely not embedded in the concrete anchorage zone. For Series 2 and 3 the bar ends were cut in a metal band saw to ensure a 90° angle at the embedded end to enable drilling and tapping the ends for instrumentation attachment and to facilitate attachment to the form work for stability during casting. A degreasing agent was applied to the bars to remove the cutting fluid residue and the bars were thoroughly rinsed with water to ensure removal of the degreaser and lubricant.

Because modern bars were used in this study instead of vintage bars, a comparison of ASTM A305-50T (*1950*) and ASTM 615A (*2005*) specifications is necessary to determine if the two bar types have similar properties. Review of the geometric and deformation requirements by Howell and Higgins (*2007*) demonstrated that the deformation requirements are identical for bar meeting ASTM A305 and modern A615 round bars. For this study, the deformation characteristics were

measured directly from the experimental bar samples. The deformation spacing was measured as 0.968 in. (24.06 mm), the deformation height as 0.0812 in. (2.06 mm), and the deformation angle as 60°. The deformation face angle was approximately 30°, and the measured diameter was 1.4115 in. (35.8 mm). To obtain these measurements, a sample was machined along the longitudinal axis of the rebar. The bar section was placed on a high resolution scanner with a reference grid, and a computer aided drafting program was used to determine the base radius. Using an average of five deformations, obtained from the sectioned bar, the base radius was determined to be 0.1817 in. (4.62 mm). The chemical composition of the bars was reported by the material supplier to be 0.44 C, 1.20 Mn, 0.19 P, 0.033 S, 0.19 Si, 0.25 Cu, 0.09 Ni, 0.16 Cr, 0.005 V, 0.028 Mo, 0.005 Nb, and 0.66 CE.

Table 2.3: Reinforcing steel mechanical properties

Test Series	f_y ksi	f_y (MPa)	f_u ksi	f_u (MPa)	% Elongation
Flexural Bars Series 1	71	(490)	106	(727)	22.5
Flexural Bars Series 2-3	66	(454)	100	(692)	26.3
Transverse Steel	54	(374)	82	(567)	29.9
Anchorage Bars	66	(453)	115	(793)	21.2

2.3.5 Specimen Construction

Formwork for the specimens was built using dimensional lumber and plywood. PVC couplers, 3 in. (76 mm) in diameter, were placed at the bottom of the forms to enable debonding of the anchorage bars from the concrete at the unloaded end of the bars. The PVC couplers were packed with dry sand to keep the anchorage bars from moving and were sealed with a silicone caulk to keep concrete paste from infiltrating the end of the reinforcing bars, as illustrated in Figure 2.7. Four tubes at each end of the specimen were used to cast voids in the column such that 1-1/4 in. (32mm) floor bolts could be used to anchor the column section to the laboratory floor during testing as seen in Figure 2.8. Two small lifting anchors were also placed in each specimen (Figure 2.5) to allow lifting and moving of the specimen. The formwork was placed on a level platform during casting to ensure orthogonal surfaces. Cover was maintained on all sides at 1.5 in. (38 mm) using slab bolsters, which were tied to the transverse reinforcement.

Figure 2.7: Typical PVC debonding pipe placed in specimens prior to casting

Concrete was placed directly from the ready mix truck into the forms as seen in Figure 2.8. Concrete was consolidated using a mechanical vibrator and the surface was finished with a hand trowel. Specimens were covered with plastic sheets and kept moist during curing. After the concrete had gained sufficient strength, the formwork was stripped and the specimens were moved to the laboratory floor for testing.

Figure 2.8: Placement of concrete into formwork

2.3.6 Test Setup

Specimens were placed on the laboratory strong floor to conduct strength tests. Wood blocks were used to provide a space between the column and floor thereby permitting access to the bottom face of the column for instrumentation. Specimens were anchored to the strong floor using 1-1/4 in. (32 mm) A193-B7 high-strength threaded rods placed 4 ft. (305 mm) on-center. To tie the specimen to the strong floor, 3/4 x 16 x 16 in. (19 x 405 x 405 mm) steel tie-down plates were used. Elastomeric bearing pads were placed between the tie-down plates and the specimen to ensure uniform contact areas as seen in Figure 2.9.

Figure 2.9: Typical Testing Setups for Series 1 and 2

A W12 x 152 loading beam with stiffeners and cutouts at anchorage bar locations was placed over the anchorage bars. The loading beam was placed on hydraulic cylinders, load cells, columns, and bearing plates as seen in Figures 2.9-2.13. Plate washers were placed between the bars and loading beam to enable uniform bearing on the loading beam, as seen in Figure 2.9. Load was transferred into the anchorage bars by means of mechanical bar couplers (Figures 2.9 and R11-R13). The mechanical bar couplers were obtained from Bar Lock International, and were designed to butt-join two #11 (36) Grade 60 (420 MPa) bars. The couplers had hex-head conically pointed bolts with heads that were specified to shear off at a torque of 410 ft-lbs (555 N-m). For this research, the bolts were tightened to 150 ft-lbs (203 N-m), and the entire coupler length was used for each anchorage bar. This permitted reuse of the bar couplers. Specimens 1M0.21, 1M0.8 and 1M0.12 were tested using a single 200 kip (890 kN) hydraulic cylinder and hollow-core load cell as seen in Figure 2.9 and Figure 2.11. Series 2 specimens were tested using the setup seen in Figure 2.9 and Figure 2.12.
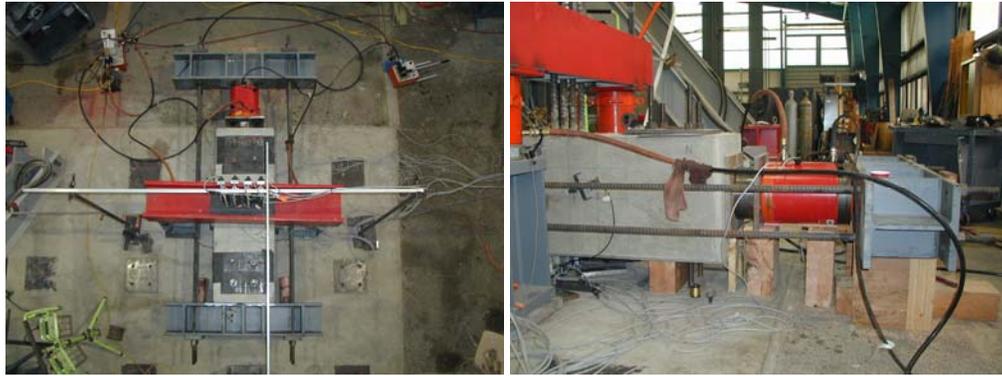
Figure 2.10: Typical plan and elevation views for Series 3

Specimens for Series 3 included a column axial compression loading setup as seen in Figure 2.10 and Figure 2.13. The axial force was self reacting on the column section. A hydraulic actuator was used to produce a compression force within the column section and reacted against a stiffened W12x120. Four high-strength (120 ksi, 827 MPa) Dywidag bars connected two W12X120 sections at the ends of the column section (Figure 2.13). The bearing area on the west end of the column shown in Figure 2.10 was 256 in^2 (0.165 m^2), while on the east face, the W12X120 was placed directly against the column with a nominal bearing area of 270 in^2 (0.174 m^2). Axial force was generated using an 800 kip (3.56 MN) hydraulic cylinder and the axial force was applied using a manual hand pump. The hydraulic cylinder, load cell, bearing plates, and W12x120's were placed on wooden blocks to insure alignment of the axial force through the geometric center of the column.
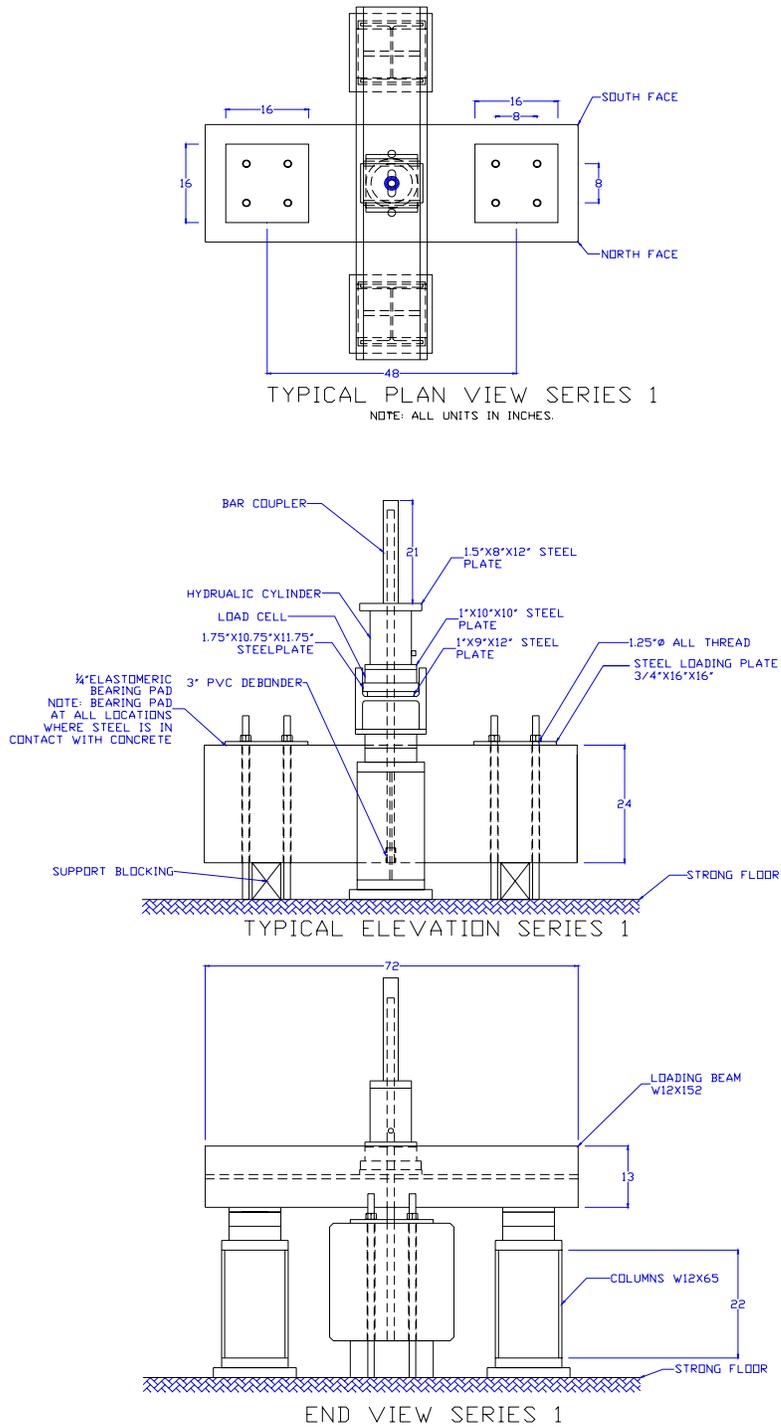
Figure 2.11: Typical Testing set up for Series 1 specimens

TYPICAL PLAN VIEW SERIES 2
NOTE: ALL UNITS IN INCHES.

TYPICAL ELEVATION SERIES 2

SECTION A-A
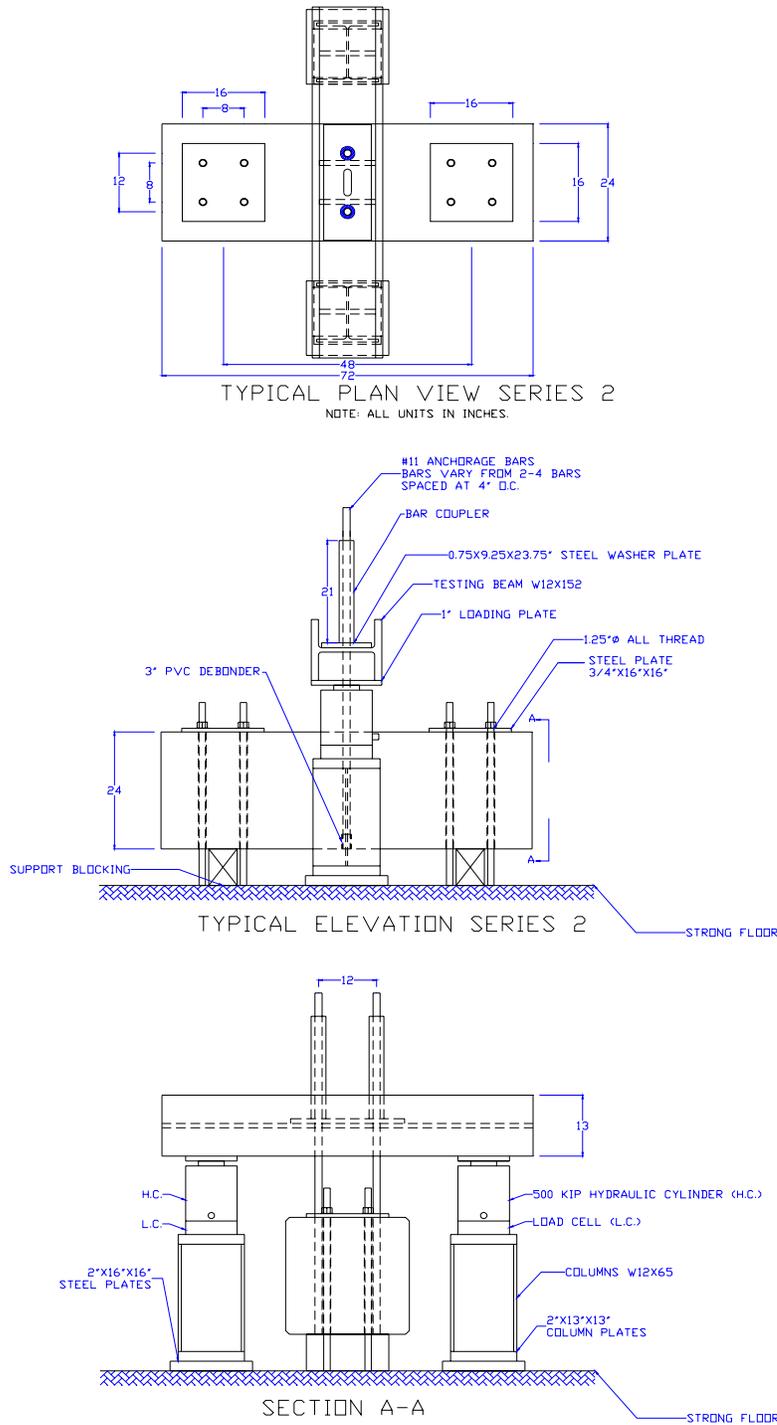
Figure 2.12: Typical testing setup for series 2 specimens (4 bar configurations not shown)

20

TYPICAL PLAN VIEW SERIES 3
NOTE: ALL UNITS IN INCHES.

TYPICAL ELEVATION SERIES 3

SECTION A-A
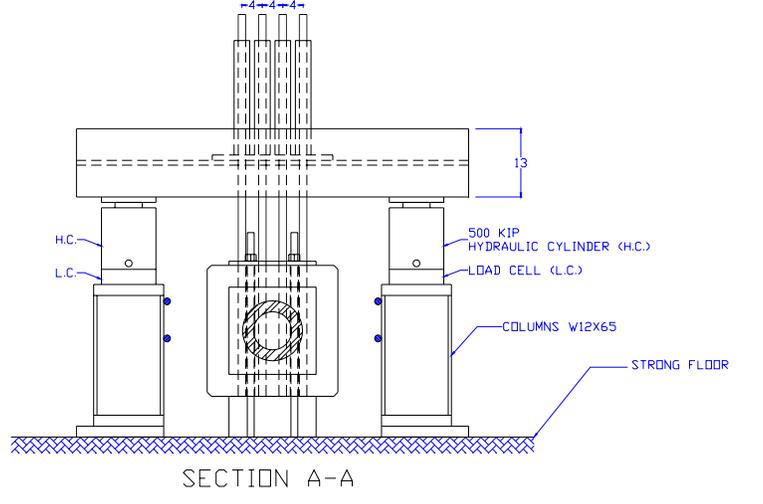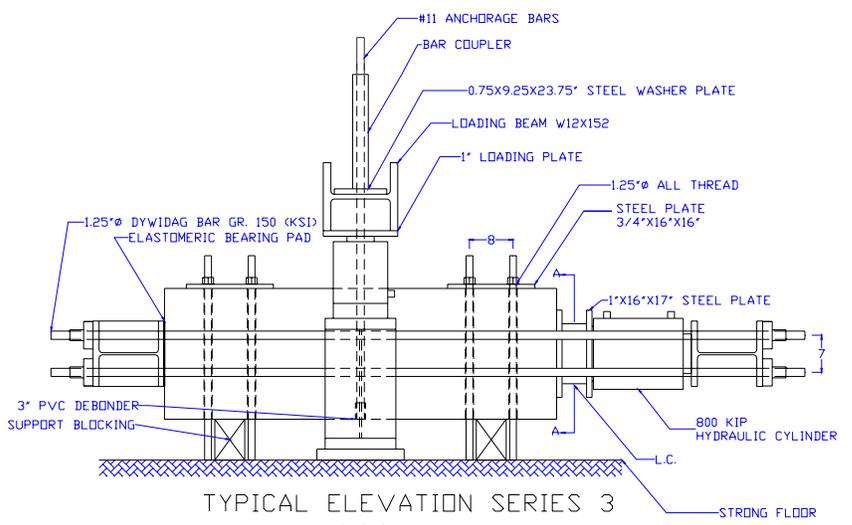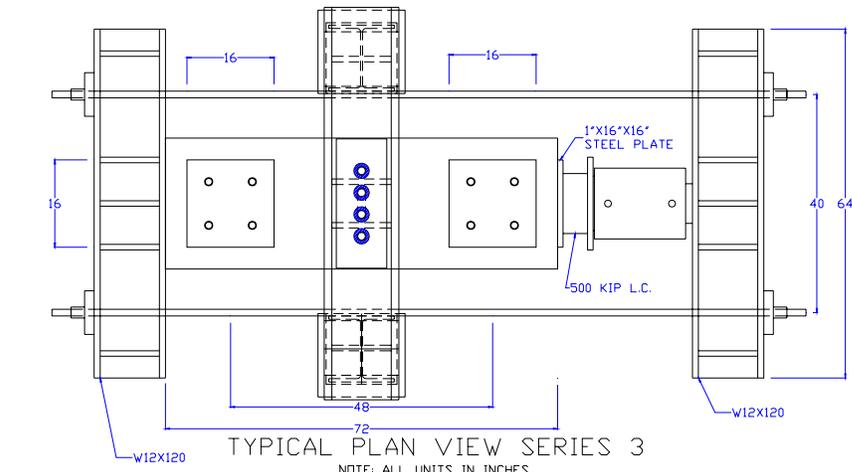
Figure 2.13: Typical testing setup for Series 3

Instruments were applied to the specimens to measure displacements, loads, and strains during testing. Typical layout of the sensors can be seen in Figure 2.14. Measurement of rigid body column motion was determined from sensors at mid-depth on the north and south sides of the column section, along with the bottom column face measurements of the specimen in-line with the anchorage reinforcing bars as seen in Figure 2.14.

TYPICAL SENSOR CONFIGURATION
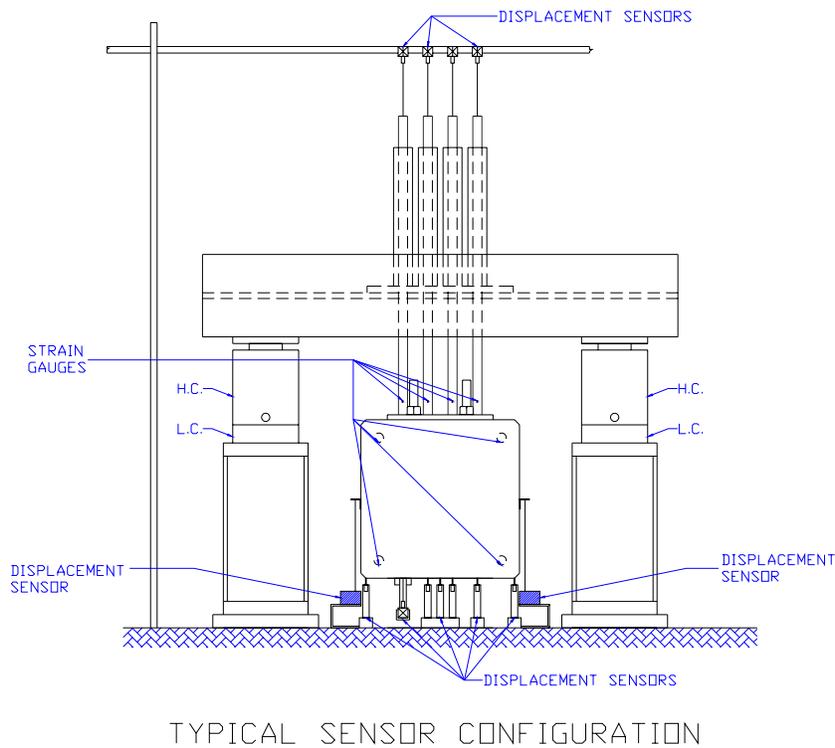
Figure 2.14: Typical sensor configuration for testing

Anchorage bar movement relative to the concrete was measured as well as overall anchorage bar displacements. Strain gauges were placed after casting on the anchorage bars at the loaded end. Strain gauges were surface bonded to the column flexural reinforcing bars prior to casting for all specimens containing four anchorage bars. The strain gauges were placed on the bottom sides of the bar to avoid damage during casting. Data from sensors were acquired and stored using commercially available PC-based data acquisition hardware and software. Data were colleted at a rate of 4 Hz and archived for subsequent data analysis.

2.3.7 Loading Sequence

The vertically applied loading consisted of a sequence of load steps applied to increasingly larger magnitude followed by unloading, throughout the duration of the test. Load was applied to achieve specified amplitudes and then held while cracks were identified and mapped and pictures were taken. The load was then released to a minimum of 1-3 kips (4.4 - 13.3 kN). Specimens were then reloaded to the next larger load amplitude. This process was continued until the specimen capacity was reached. Specimens 1M0.21, 2M0.21 and 2L0.21 were tested using 20 kip load increments. Specimens 1M0.8 and 1M0.12 were tested using 5 and 10 kip increments due to the short embedment lengths. The remaining tests were performed using 25 kip increments, except for 2L0.21, which was first loaded to 50 kips (222 kN), then the remainder of the test was performed at 25 kip load steps. Loads were controlled using a manual hydraulic pump.

Axial compression was applied to specimens in Series 3 only. Two values of axial load were used; designated as a "low" and a "high" value. The magnitude of axial load for the low value was determined from typical service level dead load on a RCDG bridge from the 1950's. Typical structural details from the Spores Bridge in the ODOT inventory (*ODOT 1957*) were used to determine the axial force in the columns from the weight of components and wearing surface. The dead weight of the bridge was calculated for the 50 ft (15.24 m) span lengths, four girder lines, 6 in. (152 mm) deck, and 2 in. (59 mm) asphalt wearing surface. A loading uncertainty factor of 5% was used to account for additional weight from other components that may have been added to the bridge, but not specified on the original plans. The service-level axial loads on the intermediate supporting columns were calculated at 200 kips (889.6 kN), and this magnitude was applied to two specimens. Anchorage demands increase as live loads are applied to the deck and girders of the bridge. These live loads also increase the axial compression in the column. To model this condition, a "high" applied axial load was selected as 500 kips (2224 kN). This was the largest amount of axial load applied to full-size bent cap specimens currently being tested at OSU. The desired axial force level was applied prior to testing and then maintained during testing.

2.4   EXPERIMENTAL RESULTS AND DISCUSSION

All specimens were tested to failure. Failure modes varied for the different specimens and included anchorage yielding, anchorage pullout, and column shear failure. Specimen behaviors were evaluated for average bond stress, maximum applied vertical load, slip of the anchorage bar, and failure mode. In addition, crack pattern and crack angle comparisons were made. Typical results of maximum applied load to the anchorage groups and slip can be seen in Figures 2.15-2.18. Maximum vertical load applied to the anchorage group at a slip of 0.005 in (0.0254 mm) and load at first slip by offset are shown in Table 4. First slip by offset was determined from visual inspection of the load-slip diagrams where a tangent line first deviates from vertical.

Table 2.4: Test results and comparison of failure modes (English Units)

Series	Specimen	Failure Mode	Axial Load At Failure (kips)	Max. Applied Vertical Load (kips)	Ave. Bar Slip at Max. Applied Load (in)	Avg. Rebar Stress at 0.005 in. Slip (ksi)	Load at 0.005 in. Slip (kips)	Avg. Rebar Stress at Load Offset (ksi)	Load at First Slip by Offset (kips)
1	1M021*	Y′	0	99	0.093	42	66#	44	69
	1M08	P+	0	46	0.165	19	30#	11	17
	1M012	P+	0	86	0.144	31	49	29	46
2	2L021	P+	0	168	0.110	19	60	30	93
	2M021	P+	0	200	0.102	32	100	37	116
	4L021	P+	0	214	0.063	20	125	17	109
	4M021	Cⁿ	0	236	0.061	12	77	9	57
3	4L221	P+	228	301	0.143	35	221	32	202
	4M221	P+	250	339	0.138	36	224	33	204
	4L521	P+	503	315	0.218	44	277	44	275
	4M521	P/Y‡	521	386	0.186	47	295	43	265

*Specimen yielded; therefore the reported values are for the load and slip just prior to yield. #Measurements were unavailable and therefore these measurements are from the loaded end at a slip of 0.01 in.

Y′ Yielding failure.

P+ Pullout failure.

Cⁿ Column shear failure.

P/Y‡ Combined yielding of bars and pullout.

Slip of the anchorage bars in the column was measured for all specimens. Slip represents the movement of the reinforcing bar relative to the rigid body motion of the concrete (*Lutz and Gergely, 1967*). A reference slip of 0.005 in. (0.127 mm) at the unloaded end of the bar was chosen for this research based on the work by Clark (*1949*). For specimens 1M0.21 and 1M0.08, the slip was obtained from the loaded end; therefore the resulting reference slip was 0.01 in (0.254 mm) Clark (*1949*). Slip was directly measured for Series 3 specimens with no further analysis, and for Series 1 and 2 the slips were calculated from separate sensor measurements as:

$$\delta_{slip} = \delta_{anchorage} - \delta_{concrete} \tag{2.3}$$

Where δ_{slip} is the movement of the reinforcing bars relative to the concrete column, $\delta_{anchorage}$ is the displacement of the particular reinforcing bar relative to the strong floor, and $\delta_{concrete}$ is the rigid body displacement of the concrete column relative to the strong floor. The rigid body displacement of the concrete column at the location of the reinforcing bars was determined from

the three bottom displacement sensors located at the bottom face of the column. A best fit line was used to determine $\delta_{concrete}$ values at the rebar locations of interest.
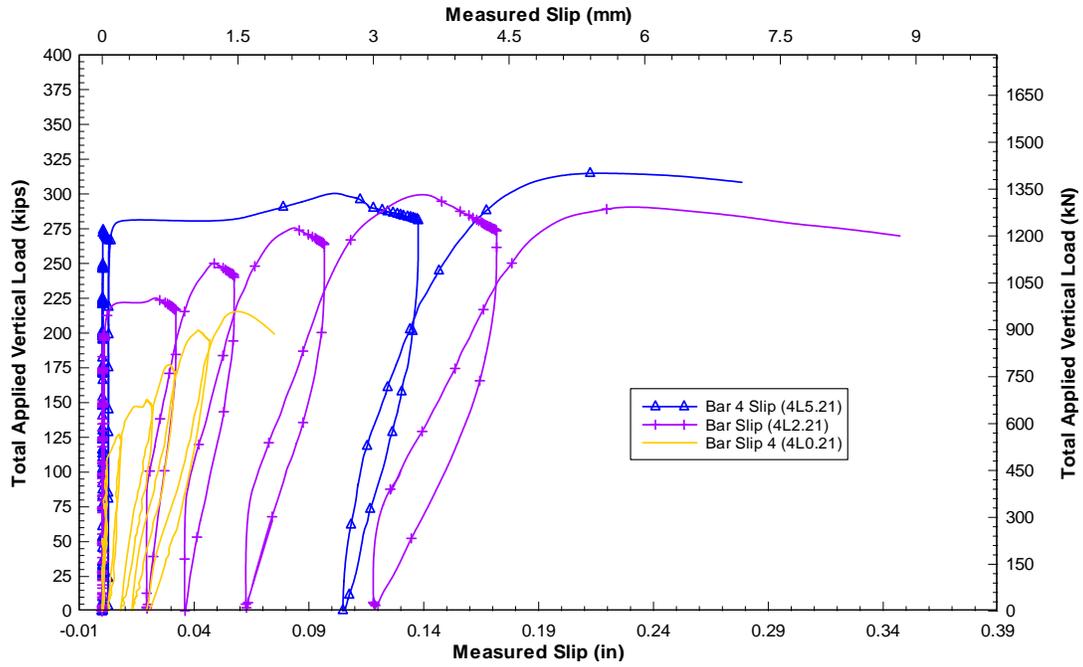
Figure 2.15: Maximum capacity comparison for outer bars of low confinement specimens
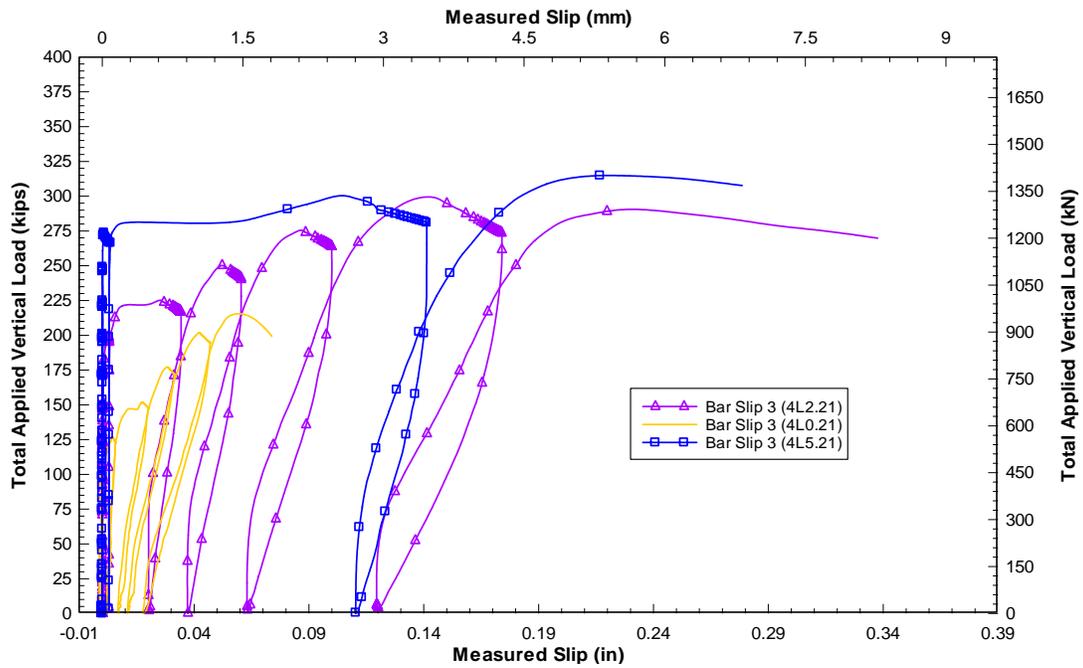
Figure 2.16: Maximum capacity comparison for inner bars of low confinement specimens
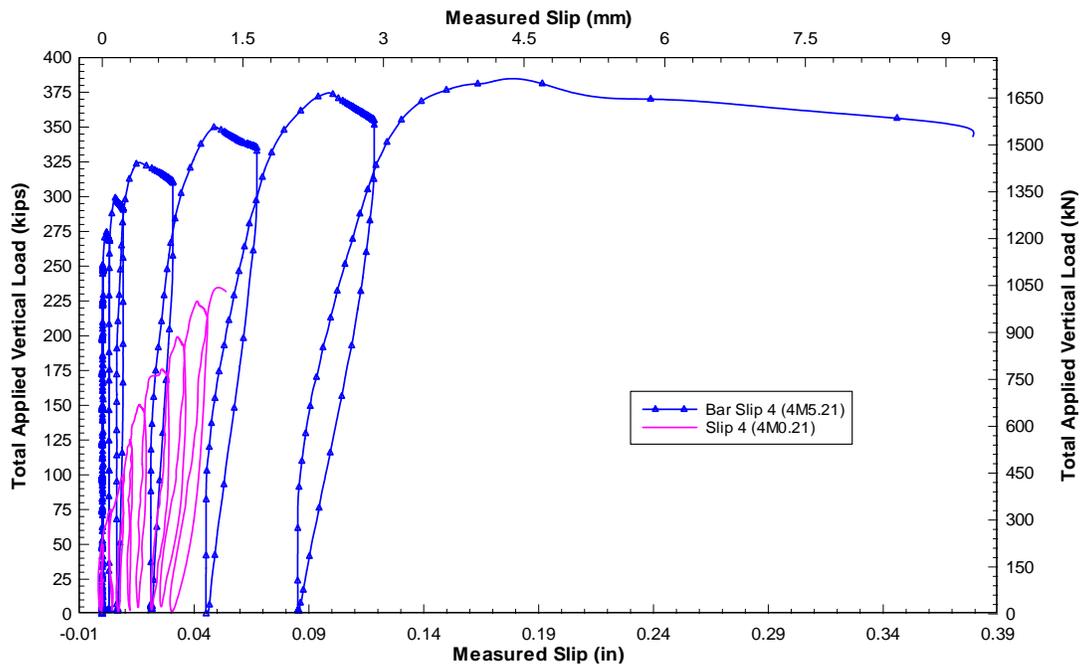
Figure 2.17: Maximum capacity comparison for outer bars of medium confinement specimens
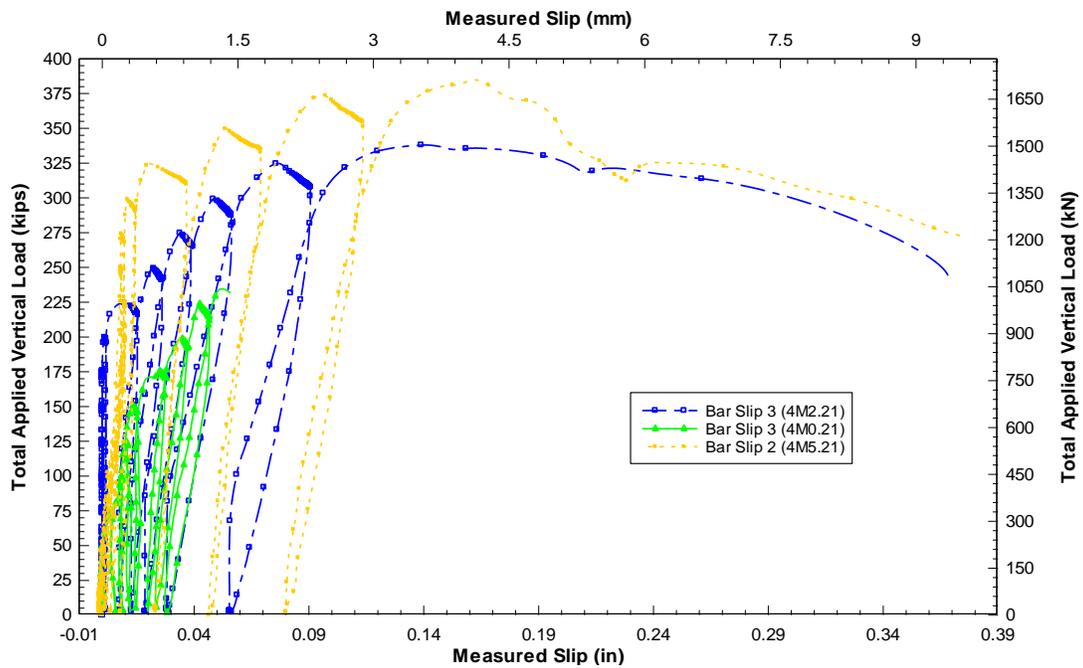
Figure 2.18: Maximum capacity comparison for inner bars of medium confinement specimens

26

2.4.1 Experimental Observations

Pullout failure of the anchorages was observed for the majority of specimens except for specimens 4M0.21, 4M5.21 and 1M0.21. Specimens in which pullout failures were observed had blocks of cracked concrete displaced along with the reinforcing bars at failure. These typically wedge shaped concrete pieces varied in size and shape based on the presence of transverse reinforcement, axial confinement, and bar configuration. Column ties tended to confine the wedge and limit the overall depth of the block to the top of the column flexural bars. For specimens without ties, the wedges were quite deep, penetrating 10 in. (254 mm) into the column (Figure 2.19 and 2.20). The concrete below the wedge and around the bar deformations showed visible signs of crushing as the bar was pulled through the concrete.

Figure 2.19: Visible concrete wedge penetration, concrete still in contact with reinforcing after failure

Figure 2.20: Failure of Specimen with concrete wedge, bar imprint visible

Transverse reinforcement increased the capacity of the specimens as seen in Table 2.4. For specimens with similar anchorage lengths, bar groupings and no axial load, the transverse confinement contributed on average an additional 27 kips (120 kN) at capacity. By adding ties, the concrete around the bar anchorage zone was better constrained and the penetration of the concrete failure planes was observed to be much shallower than that for specimens without transverse reinforcing.

The presence of axial compression in the column was seen to increase the capacity of the specimens. The axial force provided an additional 86 kips (382.5 kN) of capacity for the four-bar anchorage specimens with low confinement compared to similar specimens without axial load. The increase in anchorage strength with axial load was not proportional to the applied axial load, as increasing the axial load by a factor of 2.5 times did not increase the anchorage capacity similarly. Additionally, increasing axial load allowed for larger slip at corresponding maximum applied vertical load values as seen in Figure 2.16 and Figure 2.18. Combining axial load with transverse ties produced a mixed failure mode for Specimen 4M5.21, in which the two inner bars yielded and the two outer bars pulled out, illustrated in Figure 2.17 and Figure 2.18, where typical bar behaviors for both outer and inner bars are shown. The presence of axial force also affected the failure crack angles for Series 3 specimens. Crack angle for specimens 4L0.21, 4L2.21, and 4L5.21 were 37°, 28°, and 15°, with respect to the horizontal. For specimens with medium confinement, a similar trend in decreasing crack angle with increasing axial load is observed. Crack angles for specimens 4M0.21, 4M2.21, and 4M5.21 were 40°, 26°, and 14°, with respect to the horizontal as illustrated in Figure 2.21 - Figure 2.27.

Bar location was seen to influence the slip behavior for the reinforcing as can be seen most clearly in Figure 2.15 - Figure 2.18 where the outer bars are observed to slip more than the inner bars. This can be attributed to the interaction of the anchorage with the column reinforcing and the free edges of the column face. The edge is $4.2d_b$ away from the center of the outside bars,

and once splitting and diagonal cracks form, the outermost anchorages have reduced confinement compared to the interior bars.

LOADING KEY

—·—·—·—·—	75 kips
—·—·—·—·—	100 kips
— — — — —	125 kips
—·—·—·—·—	150 kips
—·—·—·—·—	175 kips
—··—··—··—	200 kips
—··—··—··—	225 kips
·····—·····—··	250 kips
– – – – – –	275 kips
————————	300 kips
··········	325 kips
– – – – – –	350 kips
– – – – – –	375 kips
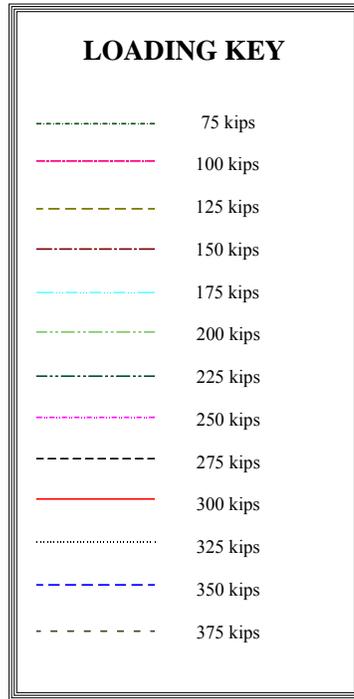
Figure 2.21: Loading legend for crack maps
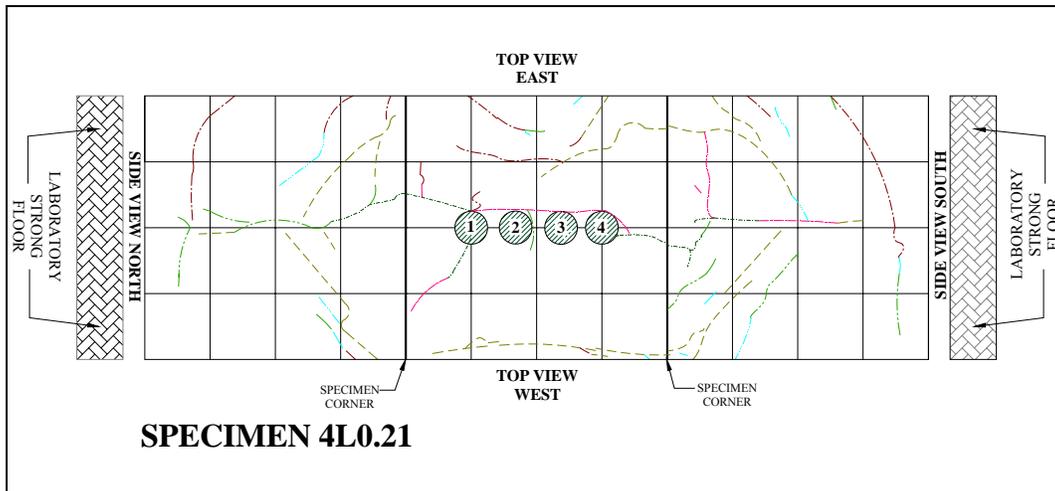
Figure 2.22: Specimen 4L0.21 crack map
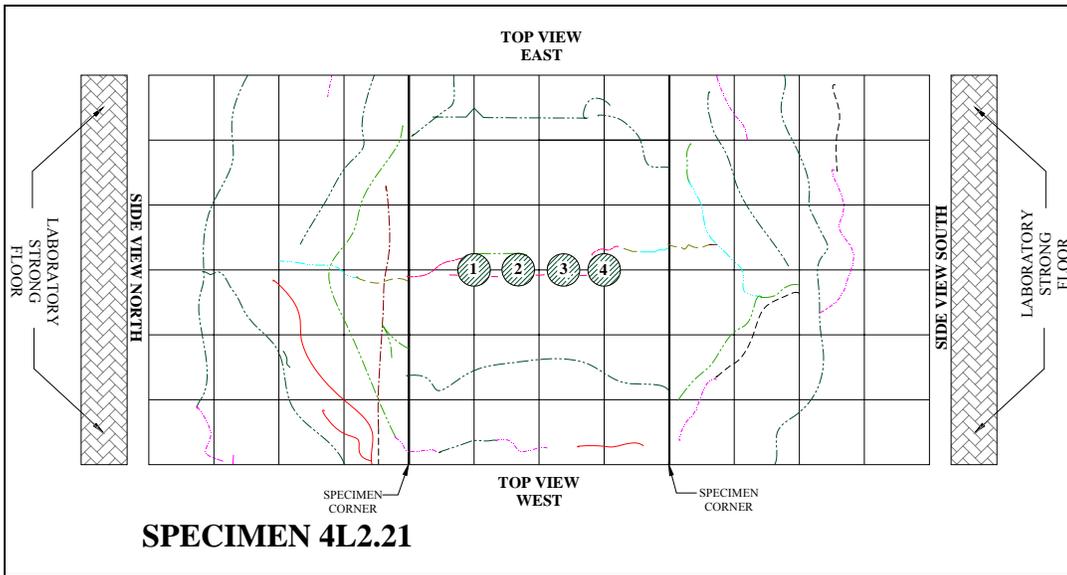
Figure 2.23: Specimen 4L2.21 crack map
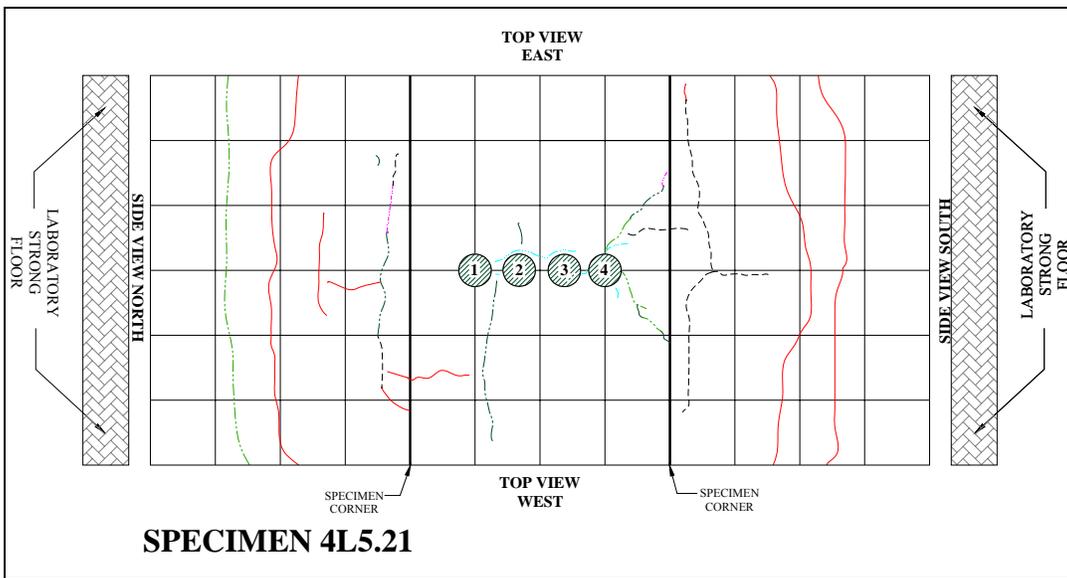
Figure 2.24: Specimen 4L5.21 crack map
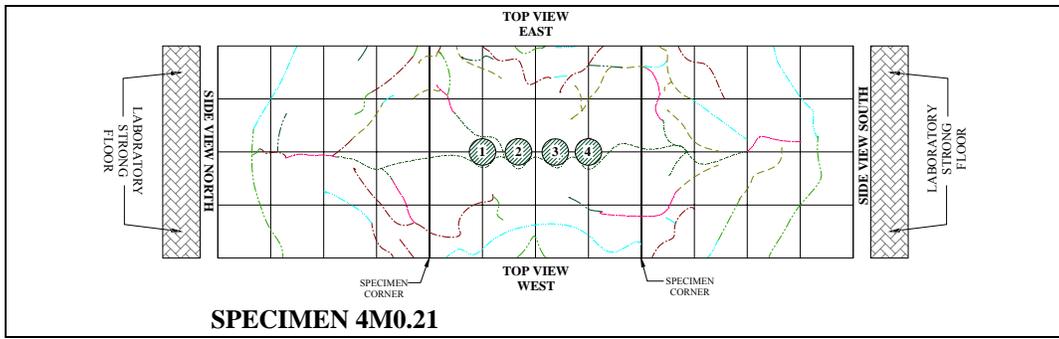
Figure 2.25: Specimen 4M0.21 crack map
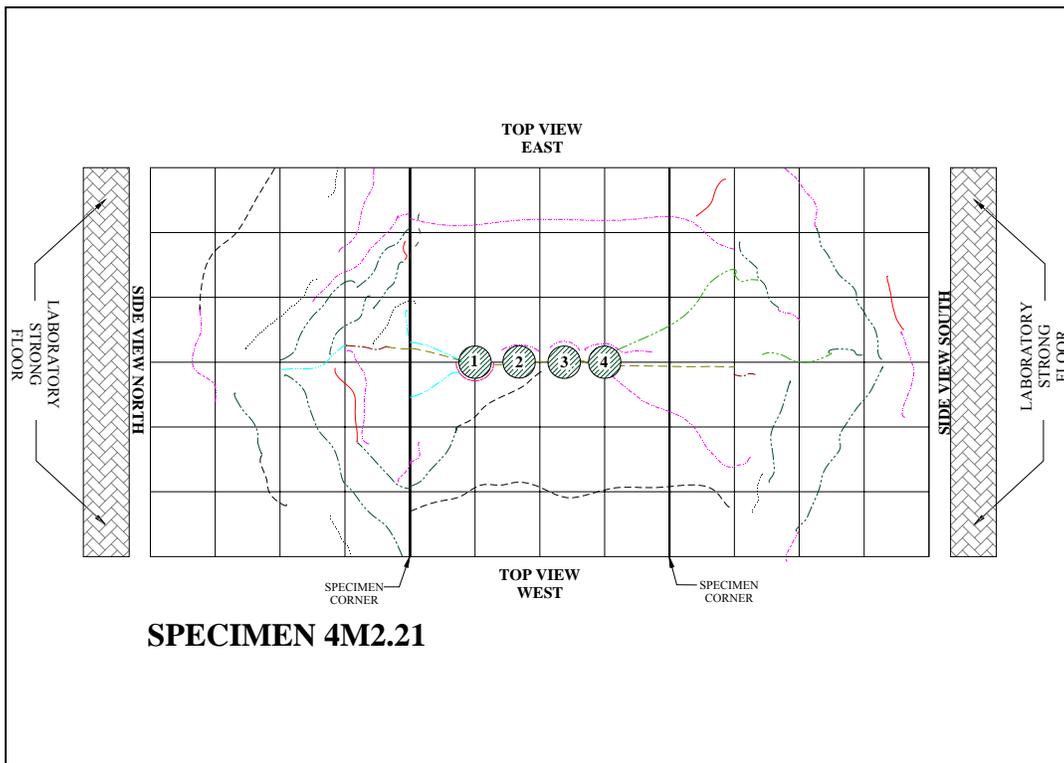
Figure 2.26: Specimen 4M2.21 crack map
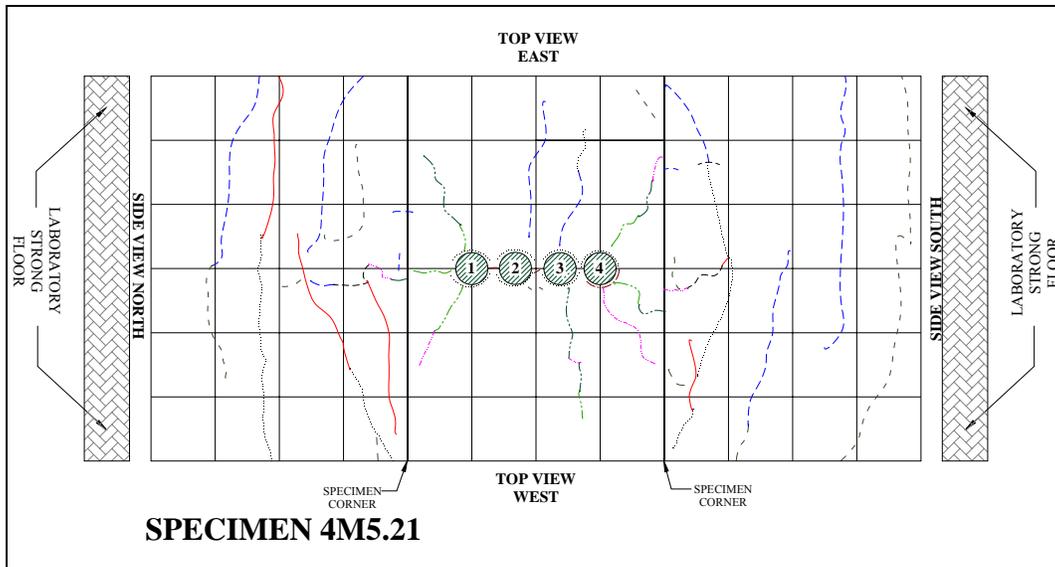
Figure 2.27: Specimen 4M5.21 crack map

2.4.2 Series Results

2.4.2.1 Series 1

Series 1 specimens consisted of single bars embedded at different anchorage lengths in the column section without axial load and with medium transverse reinforcing. The specimens produced different modes of failure depending on anchorage length provided. The cracking regions for all of specimens were generally confined to the area around the anchored bars and toward the edges of the tie-down plates used to secure the specimens to the laboratory floor. Specimens 1M0.08 and 1M0.12 failed in pullout. The magnitude of rebar stress developed for Specimen 1M0.12 was sufficient to yield a Gr. 40 ksi (275 MPa) bar, but the anchorage length of Specimen 1M0.08 was not sufficient to achieve yield for a Gr. 40 bar. Specimen 1M0.08 formed cracks at 40 kips (178 kN), very close to the maximum load of 46 kips (204 kN) seen in Figure 2.28. Specimen 1M0.12 initially cracked at 50 kips (222 kN), and subsequent cracks propagated in a radiating pattern from the bar toward the edges of the specimen and down the side faces of the column, as illustrated in Figure 2.29. Cracks did not form on specimen 1M0.21 until a load of 80 kips (355 kN), and were hairline and almost vertical as seen in Figure 2.30.

Figure 2.28: Picture of Specimen 1M08.21 prior to failure, with cracking observed

Figure 2.29: Picture of Specimen 1M12.21 near failure, with cracking observed
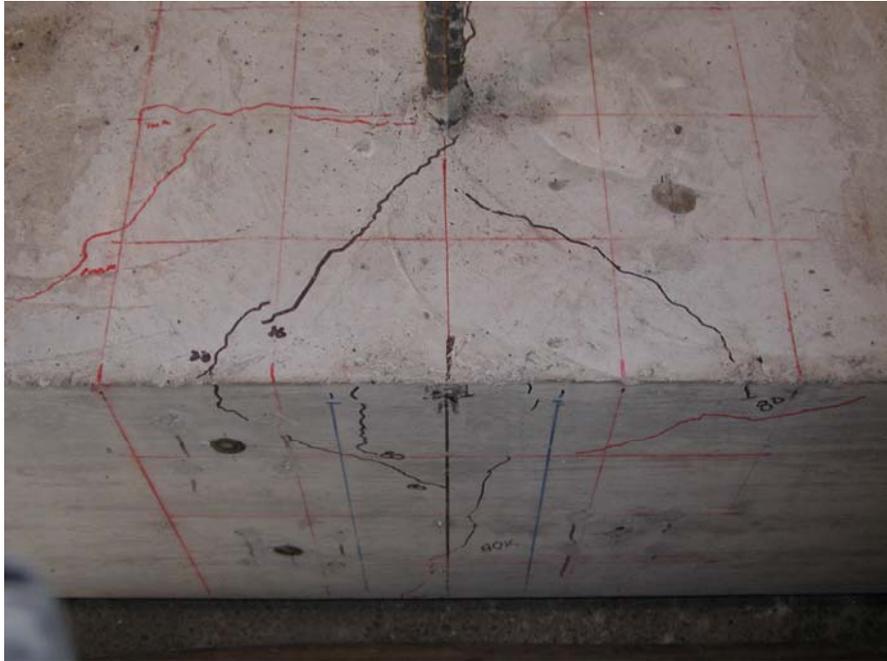
Figure 2.30: Picture of Specimen 1M0.21 at failure, with cracking observed

2.4.2.2 Series 2

These specimens contained either two or four bar groups with 21 in. (533 mm) embedment length, with and without transverse steel and no axial force. Three of the specimens exhibited pullout failures as illustrated in Figure 2.31, while Specimen 4M0.21 produced a column shear failure as seen in Figure 2.32. The maximum applied force ranged from 168 to 236 kips (747 to 1049 kN) shown in Table 4. The average bar stress for the two-bar groups at failure was sufficient to yield a similar group of #11(36) Gr. 40 (276 MPa) bars. The four-bar groups failed prior to developing stress above yield for Gr. 40 (276 MPa) bars. For anchorage specimens failing in the pullout mode, relatively large cracked wedge-shaped concrete blocks were formed (Figure 2.19 and Figure 2.20). Initial cracking for each specimen varied.
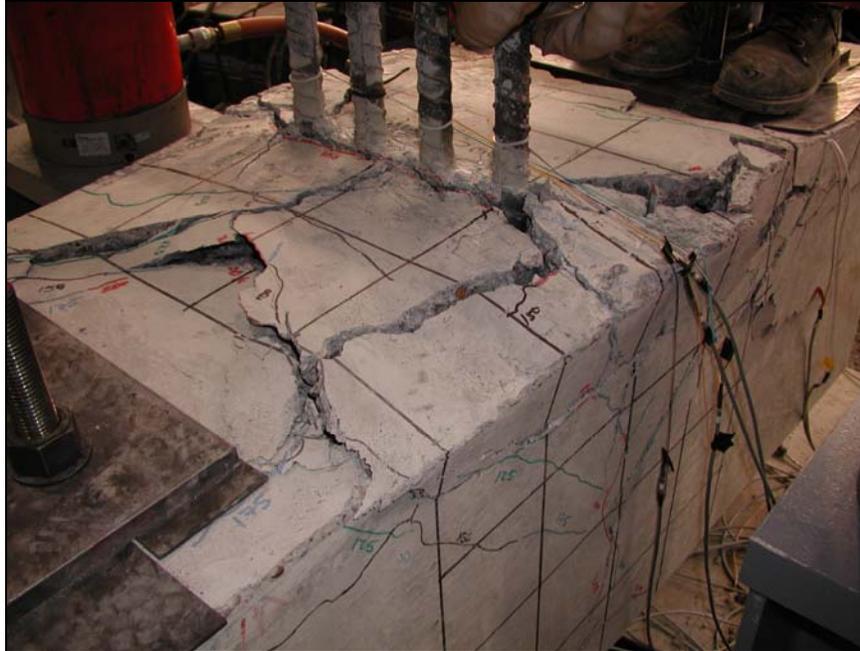
Figure 2.31: Typical pullout failure for series 2
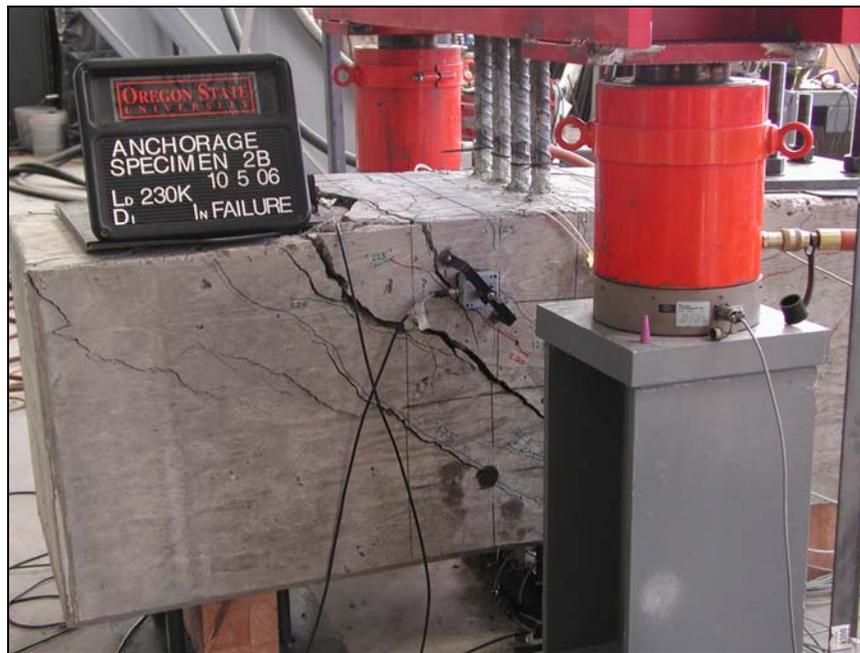
Figure 2.32: Shear failure of column section for specimen 4M0.21

For Specimen 2L0.21, initial hairline cracking was observed around the bars at 40 kips (178 kN). A large splitting crack in the plane of the bars extended down the side of the specimen at 53 kips (235 kN). At 100 kips (448 kN), diagonal cracks formed on the column side faces. Prior to failure additional diagonal cracks formed parallel to the initial diagonal cracks and progressed away from the center of the specimen. Subsequent

diagonal cracks formed deeper in the column at 150 kips (667 kN) and failure occurred in the next cycle at a maximum load of 168 kips (747 kN) with pullout of the bars and a wedge of concrete as seen in Figure 2.31.

Figure 2.33: Specimen 2L0.21 at failure

Specimen 2M0.21 exhibited initial splitting type cracking at a load of 75 kips (334 kN). This crack extended between the two bars and progressed several inches down the side faces of the column, and this initial cracking occurred at a higher load than that of specimen 2L0.21. Diagonal cracks formed at 75 kips (334 kN) and were steeper than those for the otherwise similar specimen without stirrups. This specimen was loaded to 200 kips (890 kN), at which time the specimen softened and was no longer able to carry additional load, as the rebar continued to slip relative to the concrete. The applied load was very close to yielding the bars and some flaking of the mill scale was observed. Specimen 4L0.21 exhibited initial splitting type cracking which occurred at 75 kips (334 kN), and extended down the side faces of the column section a distance of 8 in. (203 mm). At 125 kips (556 kN), diagonal cracking occurred that was similar to that observed for Specimen 2L0.21. At 200 kips (889 kN), vertical cracks on the column side faces extended to the level of the debonding PVC. Failure occurred during the next load cycle at a maximum load of 214 kips (951 kN). A large wedge of concrete pulled up with the bars, upon failure. The crack angle at failure was 37° measured from the horizontal (Figure 2.22).

36

Initial cracking for Specimen 4M0.21 also occurred at 75 kips (334 kN) and was located in the plane of the bars extending approximately halfway down the column side faces. At 100 kips (448 kN), the crack extended to just above the debonding PVC, although the specimen did not fail until 236 kips (1051 kN). Diagonal cracks formed at approximately 125 kips (334 kN). These cracks eventually became the failure plane for the one-way shear failure of the column (Figure 2.32) and formed at an angle of 40° to the horizontal (Figure 2.25).

2.4.2.3 Series 3

Specimens in Series 3 contained four bar anchorages with an embedment length of 21 in. (533 mm) and externally applied axial load to the column sections. Three specimens failed in pullout, and specimen 4M5.21 failed in a mixed mode with the inner bars yielding and the outer bars pulling out (Figure 2.17 and Figure 2.18). Measured strains for the anchorage bars are shown in Figure 2.34, where bar #1 (exterior bar) exhibited pullout with decreasing strains, whereas bar #3 (interior bar) exhibits yielding with increasing strains at failure. For Series 3 specimens failing in pullout, the maximum applied load was sufficient to yield similar groups of equivalent Grade 40 bars.
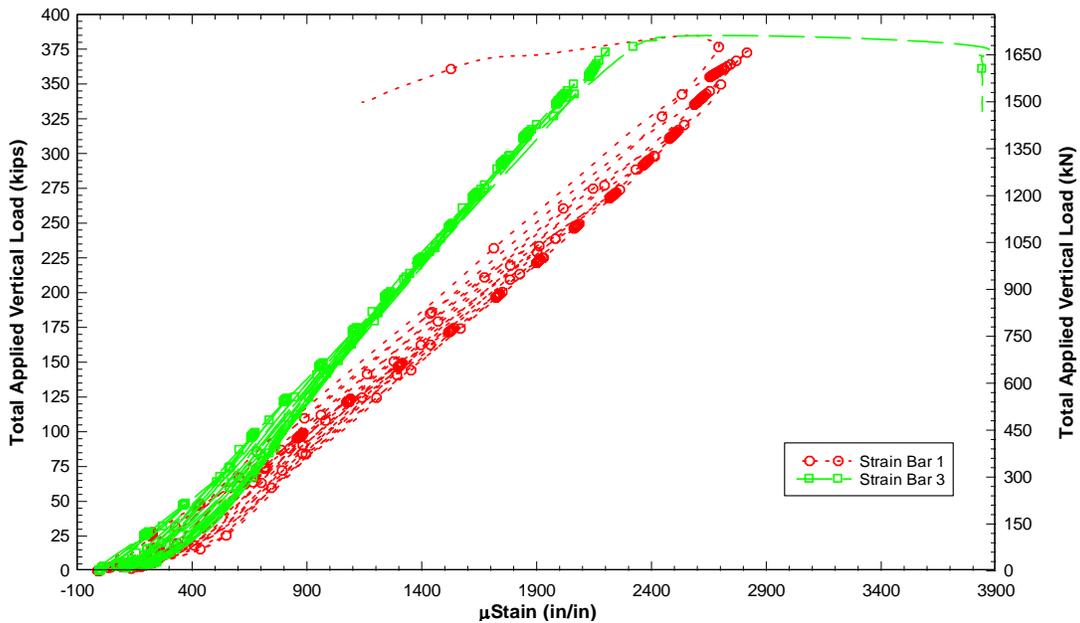
Figure 2.34: Strain for bars 1 and 3 of Specimen 4M5.21, Bar 1 pullout failure Bar 3 yielding

The load at which initial cracking was observed for Series 3 specimens was higher than that for test specimens in the previous series. Specimen 4L2.21 exhibited initial splitting cracks at 100 kips (445 kN). Diagonal cracks formed at higher loads and extended to a depth just above the debonding PVC. Diagonal cracks were considerably flatter than those from previous tests, with a crack angle of 28° with respect to horizontal (Figure 2.23). Initial cracking for Specimen 4L5.21 occurred at 175 kip (778 kN). Cracking for

this specimen was less extensive and diagonal cracks formed at failure. The diagonal crack at failure was 15° to horizontal (Figure 2.24).

Specimen 4M2.21 exhibited initial splitting cracks along the plane of the bars at a load of 125 kips (556 kN), with cracking extended 2 in. (51 mm) down the side faces of the column. The cracks at failure had a slope of 26° with respect to horizontal and extended over a large length of the specimen (Figure 2.26). Cracks reached the level of the debonding PVC, although the specimen did not fail for another 89 kips (396 kN). Cracking was more extensive in this specimen than those previously mentioned for Series 3. For Specimen 4M5.21, only minor cracking was observed around the surfaces of the bars at 150 kips (667 kN). Larger cracks did not occur until 200 kips (890 kN). Crack formation and patterns similar to those seen in Specimen 4M2.21 were observed, with vertical cracks occurring in the plane of the bars. These cracks did not propagate after 300 kips (1334 kN) stopping at a depth of 5 in. (127 mm) from the surface of the column. Crack angles for this specimen on the side face of the column were very shallow, with a crack angle of only 14° (Figure 2.27). This specimen exhibited the highest capacity in comparison to all specimens previously tested.

2.4.3 Average Bond Strength and Average Bar Stress at Ultimate Load

Average bond strength was computed for all specimens exhibiting pullout failures. Average bond strength, $\bar{f}_{bond}$ was computed as:

$$\bar{f}_{bond} = \frac{F_{max}}{n * l_d * P_o} \tag{2.4}$$

Where F_{max} is the maximum vertical force (kips) applied to the anchorage group, n is the number of bars in the anchorage group, l_d is the embedment length, and P_o is the perimeter of an individual bar. Computed average bond strengths are shown in Table 4. Average bond strength was the highest for Specimen 1M0.12. All specimens containing multiple bar groups had lower average bond strength, even as they exhibited higher overall anchorage capacities. Axial compression improved the average bond strength of the specimens, as did transverse steel as seen in Table 4. Average rebar stress at ultimate load, $\bar{f}_{s\,ultimate}$, was also used to evaluate the capacity of the anchorages, and this was computed as:

$$\bar{f}_{s\,ultimate} = \frac{F_{max}}{n * A_b} \tag{2.5}$$

Where F_{max} is the maximum applied vertical force at pullout, n is the number of bars in the anchorage group, A_b is cross sectional area of an individual reinforcing. The term $\bar{f}_{s\,ultimate}$ can be viewed as the maximum stress available from the anchorage bar just prior to failure, and is a derivation of the bond force (*Darwin, et al., 1992*).

To compare the effects of the various parameters, while reducing the variation that was present in f'$_c$, the following modification factor was applied to the ultimate rebar stress (*Baldwin and Clark, 1995*):

$$\bar{f}_{s\,(3000\,psi)} = \bar{f}_{s\,ultimate} * \sqrt{\frac{3000}{f'_{c\,experimental}}} \tag{2.6}$$

Where f'$_c$ is the experimental compressive strength of the concrete, f$_{s\,ultimate}$ is the maximum rebar stress achieved, and 3000 is the reference compressive strength (psi). It has been shown (*Darwin et al., 2005; ACI-408R-03, 2004*) that the bond strength is best characterized by $\sqrt[4]{f'_c}$, however for low strength concrete (less than 8000 psi, 55 MPa) $\sqrt{f'_c}$ is considered reasonable (*ACI-408R-03, 2004*). The average rebar stress at ultimate load, normalized by Equation 6, is shown for all specimens, failing in pullout as shown in Table 5. Average bond stresses and bar strengths for the specimens considering different transverse reinforcement, anchorage lengths, and column axial forces are shown in Figure 2.35- Figure 2.37.

Table 2.5: Normalizing f$_c$' and percent increase in capacity for column axial force and transverse steel

Specimen	f'c	√(3000/f'c)	Maximum Applied Average Force	fs ultimate	fs (3000)	% Inc. for 200 kip Axial Load	% Inc. for 500 kip Axial Load	% Inc. from 200 to 500 axial	% Inc. for Trans. Steel
	psi		lbs	ksi	ksi	-		-	-
1M08	4145	0.85	46300	29.7	25.2	-	-	-	-
1M012	4356	0.83	86000	55.1	45.7	-	-	-	-
2L021	3550	0.92	83850	53.8	49.4	-	-	-	-
2M021	3550	0.92	100100	64.2	59.0	-	-	-	19%
4L021	3786	0.89	53575	34.3	30.6	-	-	-	-
4M021	3786	0.89	59050	37.9	33.7	-	-	-	10%
4L221	3100	0.98	75175	48.2	47.4	55%	-	-	-
4M221	3000	1.00	84630	54.3	54.3	61%	-	-	15%
4L521	3200	0.97	78873	50.6	49.0	-	60%	3%	-
4M521	3100	0.98	90190	57.8	56.9	-	69%	5%	16%

In examining the column shear stress versus column bar stresses for each specimen it can be seen in Figure 2.37 where the column shear demand increased for larger bar groups, axial stress and embedment length. Also apparent is the effect of axial force in increasing the anchorage capacity. External axial force applied to the column increased the capacity of the column sections sufficiently to prevent one-way shear failure of the column, even with higher demands available from confined anchorage groups.
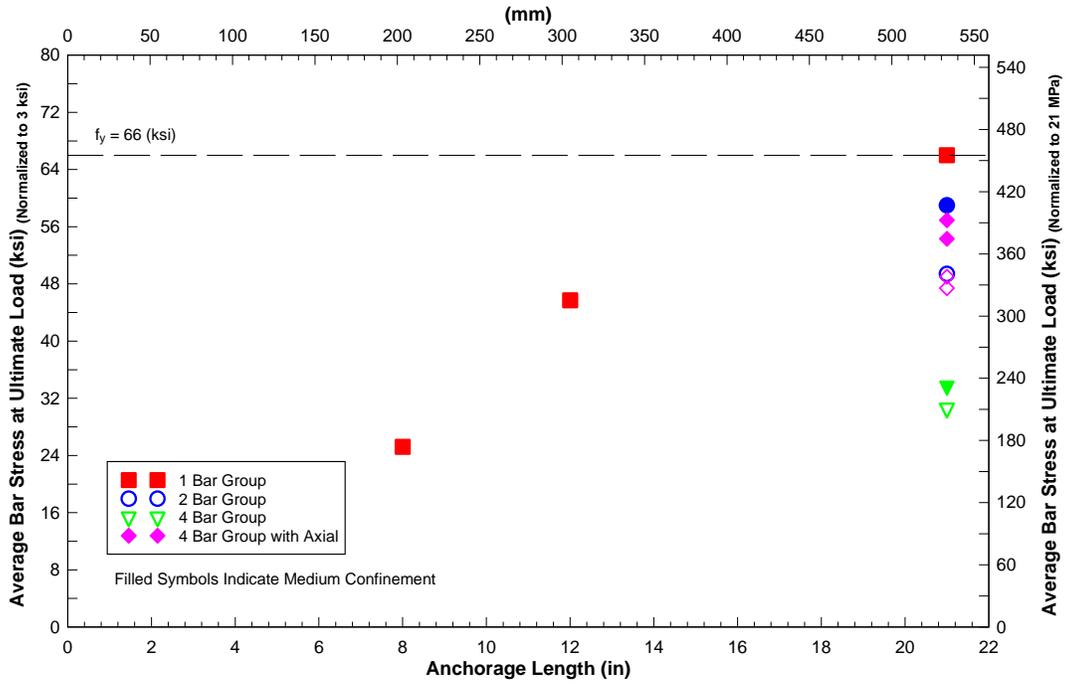
Figure 2.35: Average bar stress at ultimate load normalized to Equation 2.6 compared with anchorage length
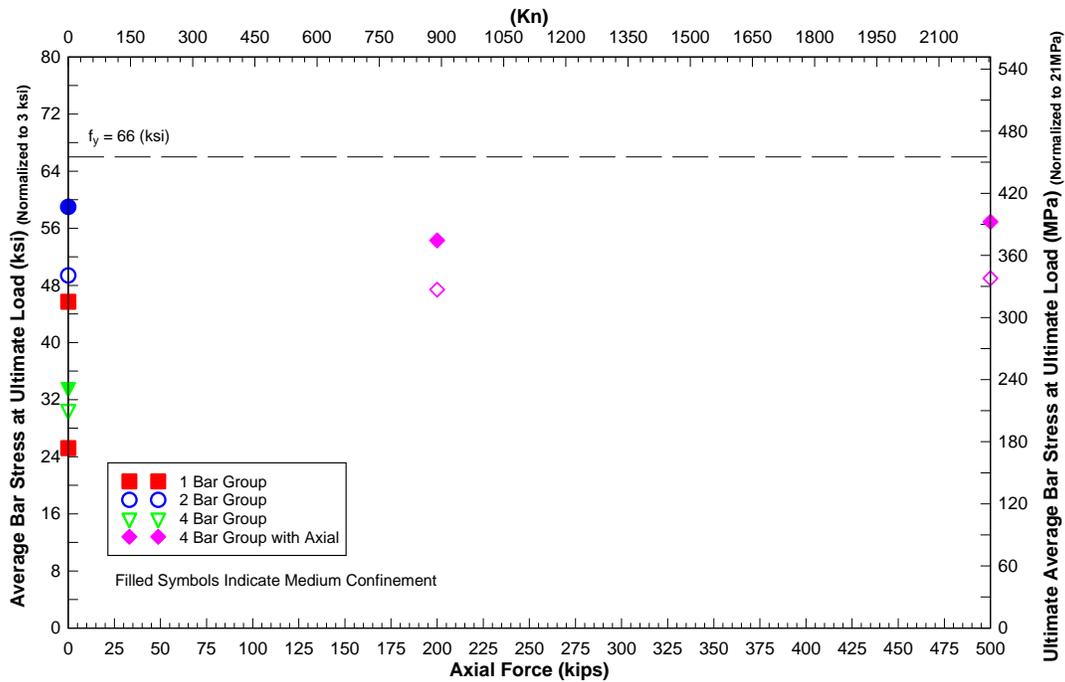
Figure 2.36: Average bar stress at ultimate load normalized to Equation 6 compared with axial force
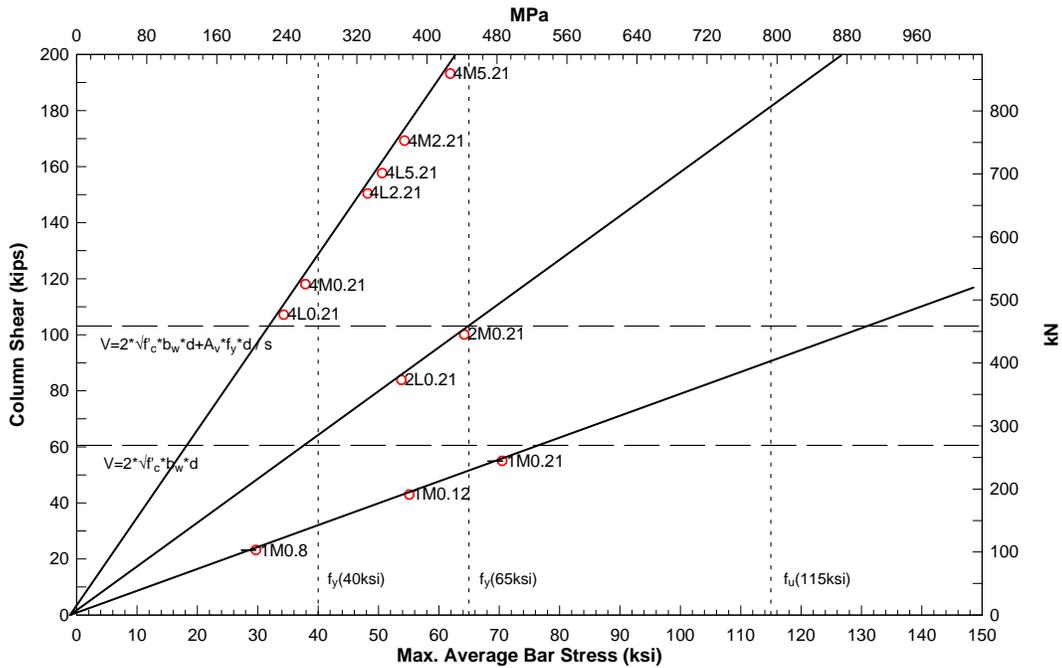
Figure 2.37: Maximum average bar stress in comparison to column shear demand

2.4.4 ANALYSIS AND EVALUATION

2.4.4.1 AASHTO LRFD and ACI318-05 Development Length Equations

The experimental data were compared to recent development length equations for straight bar anchorages from AASHTO 2005 and ACI 2005. The AASHTO 17th (*2005*) edition and AASHTO LRFD 3rd (*2005 Interim*) are identical in the methodology used to determine development length, except for the input units which are psi and ksi, respectively. The AASHTO LRFD 3rd edition will be used here.

Development length is the required length of embedment to develop the yield stress in the bar. This value is adjusted based on design parameters such as bar size, strength, coatings, and casting location. The following are equations for development from AASHTO and ACI 318-05. AASHTO section 5.11.2.1.1 calculates development length as:

$$L_{d\ AASHTO} = \frac{1.25A_b f_y}{\sqrt{f_c'}} \qquad (2.7)$$

Where A_b is the area of the reinforcing being developed (in^2), f_y is the nominal yield strength (ksi) and f_c' is the design concrete compressive strength (ksi). The development length must be taken larger than:

41

$$L_{dmin\ AASHTO} = 0.4d_b f_y \qquad\qquad (2.8)$$

Where d_b (in.) is the diameter of the bar and f_y (ksi) is the yield stress, and the above two equations are applicable only to #11 (36) bars and smaller. ACI 318-05 section 12.2.3 requires development length be calculated as:

$$L_{d\ ACI} = \left(\frac{3}{40} \frac{f_y}{\sqrt{f'_c}} \frac{\psi_t \psi_e \psi_s \lambda}{\left(\dfrac{C_b + K_{tr}}{d_b} \right)} \right) d_b \qquad\qquad (2.9)$$

Where d_b is the diameter of the bar (in.), f_y is the yield stress (psi), f'_c is the compressive concrete strength (psi), ψ_t ψ_e ψ_s are coefficients for top bar effects, epoxy coating, and bar size effects, respectively, which for this analysis are taken as 1.0. The factor λ is used for either normal or light-weight concrete. In this research only normal weight concrete was used, and thus λ was taken as 1.0. The C_b term is defined as the least dimension of either the distance from the center of the bar to nearest concrete surface or one-half the center-to-center spacing of the bars being developed. The term K_{tr} accounts for the effects of transverse reinforcement against splitting and is calculated as:

$$K_{tr} = \frac{A_{tr} f_{yt}}{1500sn} \qquad\qquad (2.10)$$

Where A_{tr} (in^2) is the area of transverse steel, f_{ty} (psi) is the yield stress of the transverse reinforcing, s (in.) is the center to center spacing of the transverse reinforcing, and n is the number of bars being developed in the plane. In ACI 318-05 the term K_{tr} can be taken as 0 and the term $(K_{tr} + C_b)/d_b$ can be no larger than 2.5, to ensure that for developed or spliced bars a splitting failure governs over a pullout failure (*ACI 408R-03, 2004*).

2.4.4.2 Development Length to Average Bar Stress

Experimental results for average ultimate bond strength and maximum average bar strength were used to compare with the previously described methodologies for predicting the capacity of the flexural bar anchorages in column sections. AASHTO LRFD and ACI 318-05 as seen previously do not provide a means of explicitly evaluating anchorages in the presence of confining axial loads, and modifications are proposed to account for this beneficial effect.

ACI and AASHTO rely on ultimate strength design limit states and define a development length required to produce yielding of the bars at ultimate strength. This does not provide a means of directly evaluating ultimate bond strength. However, comparisons between the experimental results and the available analysis methods were made by taking a ratio of the experimentally provided anchorage length to the specified anchorage length computed from the analysis methods. Multiplying this ratio by the yield stress of the

embedded reinforcing bar determines the fraction of the rebar stress predicted by the provided embedment. As shown in ACI 408R-03 (*2004*) and Baldwin and Clark (*1995*), increasing the embedment length does not proportionately increase the bond strength, but the relationship is reasonably close to a linear force transfer and thus may be expected to provide reasonable results. Ratios of the experimental bar stress to predict bar stress were computed, which show that when this value is less than 1.0 the predicted bar stress is greater than the experimentally measured value and when greater than 1.0 the predicted bar stress is smaller than the experimentally measured value.

2.4.4.3 Code Prescribed Inputs

Each specimen had distinct geometric and structural parameters which were applied to the various development length equations. AASHTO development length variables were the concrete compressive strength and reinforcing strength (Equation 2.7) and results are shown in Figure 2.38. For ACI 318-05, initial comparisons were performed for each specimen depending on the value of $(C_b+K_{tr})/d_b$. The impact of K_{tr} was evaluated but the influence of C_b was not examined as this varies only with the spacing and cover geometry of the specimen, which did not vary substantially for the different specimens with rebar groups. However, in cases with only one bar, C_b was taken as the distance from the center of the bar to the side face of the concrete column. Initially three evaluations of the influence of K_{tr} where made, as seen in Table 6. These where: K_{tr} equal to zero as the default value and as a conservative assumption permitted by ACI 318-05, K_{tr} equal to the value calculated in Equation 10 with code imposed limitations for $(C_b + K_{tr})/d_b$, and finally $(C_b + K_{tr})/d_b$ not limited by the code upper limit only for those specimens with superimposed axial compression. The variables for K_{tr} seen in Eqn. 10 refer to transverse steel resisting splitting along the plane of the bars. In the application of this equation, the #11 (36) flexural (column) bars were used for A_{tr} with their corresponding yield value (60) ksi (414 MPa) for f_{tr}. The variable n reflected the number of bars being pulled in the anchorage group. The variable s was originally defined as the stirrup spacing, however, the anchorage bars are parallel to the ties and the column flexural bars act as the transverse reinforcing to the splitting plane, thus the internal flexural lever arm jd (in.) was used for the value s. The internal flexural lever arm was calculated from equilibrium and strain compatibility at the strength limit state using elasto-plastic steel and Whitney stress block material assumptions.

The experimental and predicted bar stresses by the above method are shown in Figure 2.38-Figure 2.39. The values of the calculated development length are shown in Tables 2.6 and 2.7. The data used for all development length equations are contained in Appendix A.
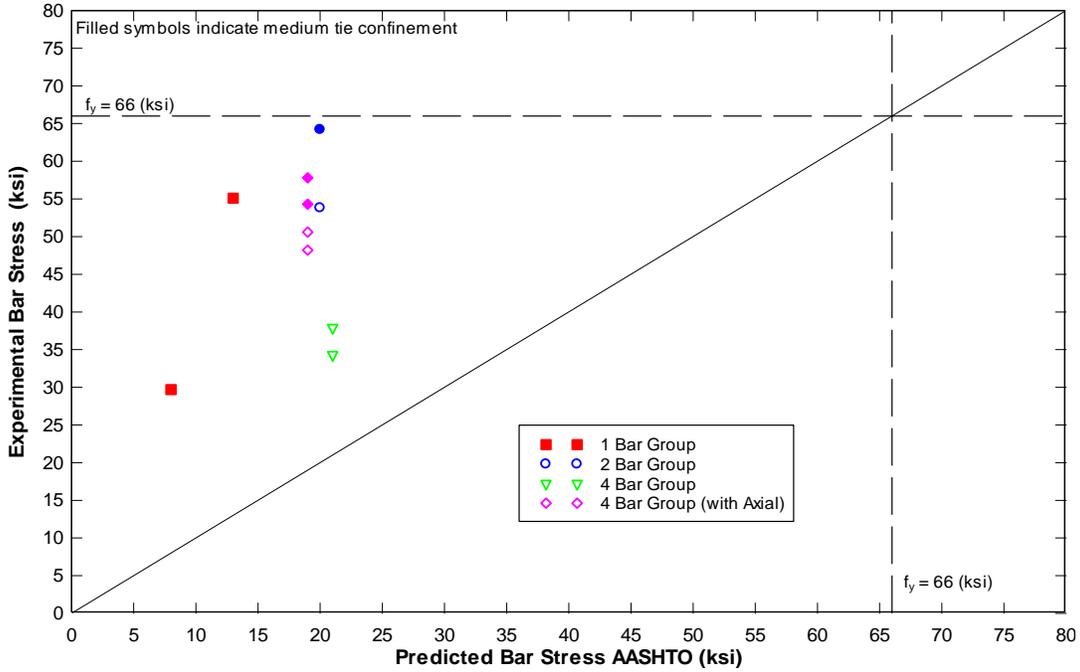
Figure 2.38: Experimental bar stress in comparison to AASHTO predicted bar stress
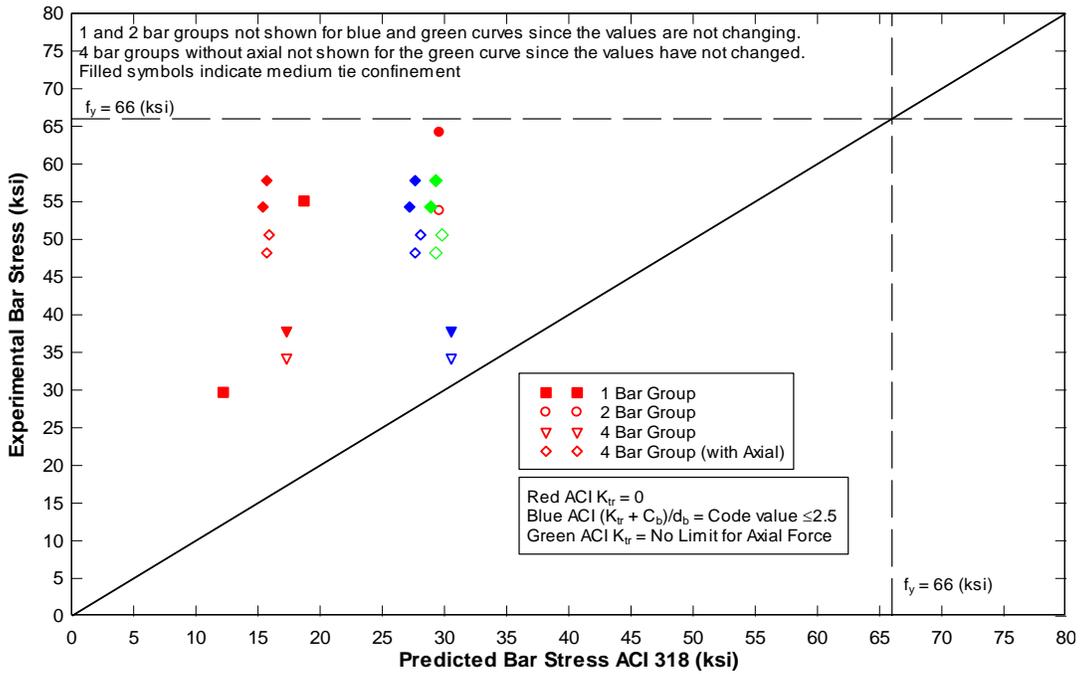
Figure 2.39: Experimental bar stress in comparison to ACI 318-05 predicted bar stress

As seen in Figure 2.38 the AASHTO method is quite conservative with minor variation due only to f'$_c$. ACI 318-05 reasonably predicted the capacity of the four bar specimens without axial load when using calculated K_{tr} while four bar specimens with axial were predicted with considerable conservation as seen in Figure 2.39. When removing the

44

upper limit applied to the contribution from stirrups and cover for the benefit of axial force, little difference in the values is observed. Therefore to eliminate some of the conservatism found when evaluating 1950's vintage straight bar anchorages, a modifying term is developed in the following sections to account for the beneficial presence of transverse pressure.

Table 2.6: Development lengths for AASTHO and ACI $_{(Ktr = 0)}$

Spec. Name	AASHTO				ACI $_{(Code\ Calculated\ Value\ with\ (Cb + Ktr)/db = 0)}$						
	L_d (in)	L_{exp}/L_d	f_s (ksi)	f_s Exp. / Pred.	K_{tr}	$(C_b + K_{tr})/d_b$	$(C_b + K_{tr})/d_b \leq 2.5$	L_d (in)	L_{exp}/L_d	f_s (ksi)	f_s Exp. / Pred.
1M08	63	0.13	8	4	0	8.51	2.50	43	0.18	12.2	2.4
1M012	62	0.19	13	4	0	8.51	2.50	42	0.28	18.7	2.9
2L021	68	0.31	20	3	0	4.26	2.50	47	0.45	29.6	1.8
2M021	68	0.31	20	3	0	4.26	2.50	47	0.45	29.6	2.2
4L021	66	0.32	21	2	0	1.42	1.42	80	0.26	17.3	2.0
4M021	66	0.32	21	2	0	1.42	1.42	80	0.26	17.3	2.2
4L221	73	0.29	19	3	0	1.42	1.42	88	0.24	15.7	3.1
4M221	74	0.28	19	3	0	1.42	1.42	90	0.23	15.4	3.5
4L521	72	0.29	19	3	0	1.42	1.42	87	0.24	15.9	3.2
4M521	73	0.29	19	3	0	1.42	1.42	88	0.24	15.7	3.7

Table 2.7: Development length results for ACI 318-05

Spec. Name	ACI $_{(Code\ Calculated\ Value\ with\ (Cb + Ktr)/db \leq 2.5)}$							ACI $_{(Limit\ applied\ to\ specimens\ without\ axial\ force\ only)}$					
	K_{tr} (in)	$(C_b + K_{tr})/d_b$	$(C_b + K_{tr})/d_b \leq 2.5$	L_d (in)	L_{exp}/L_d	f_s (ksi)	f_s Exp./ Pred.	K_{tr} (in)	$(C_b + K_{tr})/d_b$	L_d (in)	L_{exp}/L_d	f_s (ksi)	f_s Exp./ Pred.
1M08	7.4	13.8	2.5	43.4	0.2	12.2	2.4	7.4	13.8	43.4	0.2	12.2	2.4
1M012	7.4	13.7	2.5	42.3	0.3	18.7	2.9	7.4	13.7	42.3	0.3	18.7	2.9
2L021	3.4	6.7	2.5	46.9	0.4	29.6	1.8	3.4	6.7	46.9	0.4	29.6	1.8
2M021	3.4	6.7	2.5	46.9	0.4	29.6	2.2	3.4	6.7	46.9	0.4	29.6	2.2
4L021	1.7	2.6	2.5	45.4	0.5	30.5	1.1	1.7	2.6	45.4	0.5	30.5	1.1
4M021	1.7	2.6	2.5	45.4	0.5	30.5	1.2	1.7	2.6	45.4	0.5	30.5	1.2
4L221	1.7	2.7	2.5	50.1	0.4	27.6	1.7	1.7	2.7	47.2	0.4	29.3	1.6
4M221	1.7	2.7	2.5	51.0	0.4	27.2	2.0	1.7	2.7	48.0	0.4	28.9	1.9
4L521	1.7	2.7	2.5	49.4	0.4	28.1	1.8	1.7	2.7	46.5	0.5	29.8	1.7
4M521	1.7	2.7	2.5	50.1	0.4	27.6	2.1	1.7	2.7	47.2	0.4	29.3	2.0

2.4.5 Proposed Modification to Anchorage Development Length Due to Column Axial Confinement

The above code prescribed methods provided overly conservative estimates of anchorage capacity for the specimens, including, in particular, those specimens with axial load at service-level magnitudes. In an effort to establish a more reasonable prediction of flexural anchorage capacity in column-bent connections with applied axial compression under gravity loads, a modification to the ACI 318-05 approach is proposed. The modification takes into account active confinement from the column axial compression stress acting across the potential anchorage splitting plane. AASHTO LRFD was not evaluated since this approach has been seen to be the least conservative (*Darwin 2005*), and is based on less robust methodology and does not include many important variables (*Orangun et al. 1977; Darwin 2005*).

Data from the present research, along with Elighausen *et al*. (*1983*), Untrauer and Henry (*1965*), and Robins and Standish (*1982*) and Batayneh (*1993*) were combined to develop a modification factor for development length prediction that accounts for the column confining pressure. Confining pressure and other modeling input data were determined from reported figures and tables. The specimens in which yielding occurred were eliminated from the analysis, along with specimens in which the lateral pressure applied was greater than $0.3f_c$, which was on average observed to be the upper limit of the benefit seen from adding transverse pressure Robins and Standish (*1984*); Nagatomo and Kaku (*1992*); Walker *et al*. (*1997*). For each individual specimen, the ACI 318-05 development lengths were calculated. The term K_{tr} was taken as zero for the development of the modifying term since it was seen that the benefit of axial pressure was substantially larger than that of the column reinforcing, therefore ignoring their contribution is conservative. The term $(1/(C_b/d_b))$ was still limited to a maximum value of 2.5. The ACI 318-05 computed development length was divided by the experimentally provided embedment length and this was then multiplied by the yield stress to produce a predicted rebar stress. The predicted rebar stress was then compared to the experimentally reported stress. The ratio of predicted to actual rebar stress along with applied column pressure (acting transverse to the splitting plane) was evaluated. A best fit curve was determined by performing a nonlinear regression of the data. Assuming a normal distribution for the data, confidence intervals were established. The best fit curve and the confidence intervals are shown in Figure 2.40. As seen here, the best fit curve is approximately linear with respect to the column axial compression stress. Considering the 95% lower bound confidence level and approximating it as linear, a best fit modification factor was established as:

$$\kappa = 0.8 + \frac{p}{800} \leq 2.25, \geq 1.0 \tag{2.11}$$

Where p is taken as the service-level column compression stress (psi) on the gross column cross section acting transverse to the anchorage splitting plane. An upper bound of 2.25 was selected (approximately $p<0.3f_c$ for lower strength concrete) due to limitations in the data at very high compression stresses and prior research results. A lower bound of 1.0 provides that axial compression stresses below 160 psi (1.1 MPa) are not relied upon to provide reduced development length.

The modification factor κ implementation can be seen in the adjusted ACI 318-05 development length equation:

$$L_{d\ \text{ACI Modified}} = \left(\frac{3}{40} \frac{f_y}{\sqrt{f_c'}} \frac{\psi_t \psi_e \psi_s \lambda}{\left(\dfrac{C_b}{d_b} \right) * \kappa} \right) d_b \qquad \textbf{(2.12)}$$
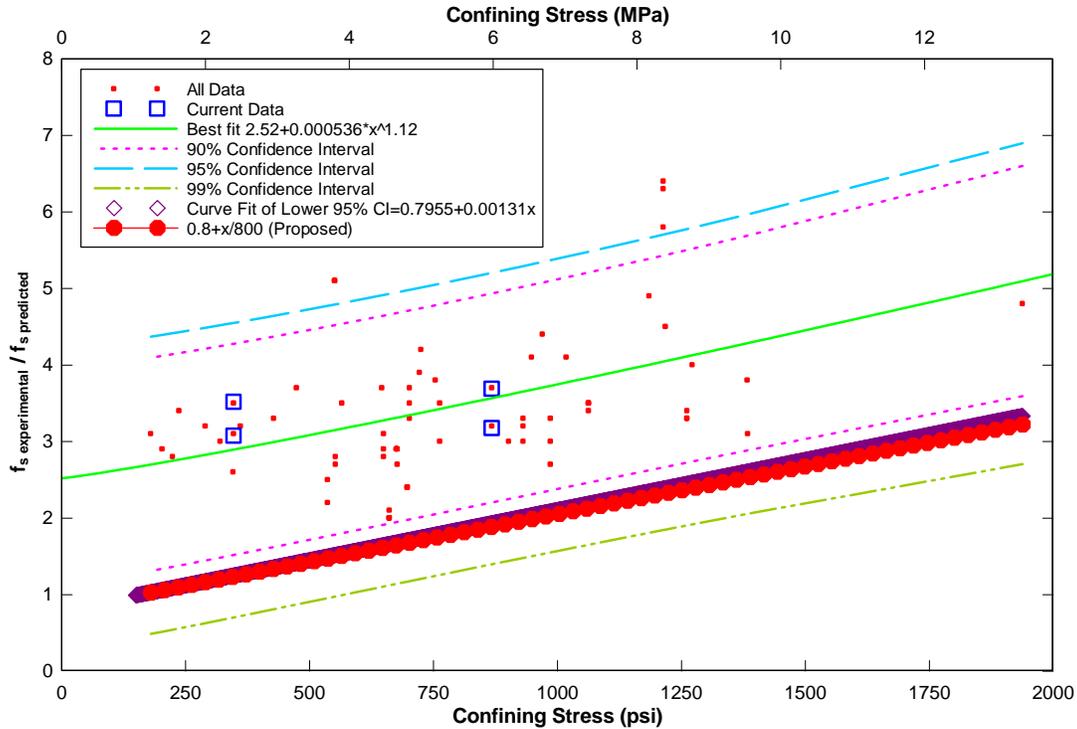
Figure 2.40: Actual to predicted rebar stress interaction with column axial stress transverse to the splitting plane

2.4.6 CEB-FIP Recommendations

In evaluating the proposed method, a comparison was made with the CEB-FIP Recommendations (CEB-FIP) which includes a reduction factor to account for the presence of compressive transverse stress across the splitting plane of the developing bars. CEB-FIP Recommendations Section 2.4.1.5 describes the reduction factor as follows:

$$\frac{1}{(1-0.04p)} \leq 1.5 \qquad \textbf{(2.13)}$$

Where p is the pressure transverse (MPa) to the plane of reinforcement. This term is applied as an increase to the design bond strength and can be taken as 3/2 at an end anchorage. While it may appear that Equation 2.11 is less conservative than Equation 2.13, the CEB-FIP procedures

produce shorter straight bar anchorage lengths than those in ACI 318-05. Comparing the simplified development length equations in ACI 318-05 for #7 (#22) and larger bars with clear spacing of at least a bar diameter and at least minimum stirrups against that in section 2.4.1 of CEB-FIP Recommendations considering 36 mm diameter bars, over a range of concrete compression strengths from 3000 to 5000 psi (20 to 35 MPa), the CEB-FIP Recommendation anchorage lengths are on average 1.44 time shorter than those by ACI. As a result, at the limiting values of Equation 11 and Equation 13, the proposed approach is only about 3% higher than the CEB-FIP Recommendations and produces about the same anchorage lengths. At lower column axial stresses, the proposed method with Equation 11 would result in higher predicted anchorage lengths than those from CEB-FIP. It should be noted that the proposed modification factor κ, developed using ACI 318-05 as Equation 12 allows a significant reduction in development length than currently permitted and is limited to applications for existing structures under gravity loading containing materials, details, and proportions like those considered here rather than for new design.

2.5   LIMITATIONS

The research conducted was directed toward evaluation of 1950's flexural bar anchorages in bent cap columns. The research results were not developed for application to new designs. The column sections employed were realistic sized sections but represent only one size, reinforcing scheme, and concrete mix design. It was seen that the main column flexural bars did not achieve yield and although outside the scope of this research, the column bar contribution could be further investigated to determine the influence of other column steel reinforcing patterns on anchorage behavior.

3.0   CONCLUSIONS

Tests were conducted on 1950's vintage column-bent specimens to determine the influence of different bar groupings, axial load, and transverse steel parameters on the strength of flexural bar anchorages terminating in columns. Eleven anchorage tests were performed. Specimen results were reported and compared with current bridge and building design specifications. An active confinement term was developed for the analysis techniques currently in practice, and anchorage predictions were compared with results from previous experimental research. Based on the reported research, the following conclusions are made:

- The subassemblage specimens provided a reasonable approximation of the details for 1950's vintage flexural anchorages terminating in columns. The stress state in the tested column section is conservative when compared with complete bent cap members, due to the presence of bending in the column subassemblage and shear that are not observed in full-size bent caps.

- Bar location affected the slip and capacity of bars, with those located near the free edge of the specimen exhibiting reduced capacity. These outer bars also tended to have larger slip values and less stiffness than those located in the center of the column section.

- The presence of multiple bars decreased the average maximum bond stress. The bar stress was lower for the four-bar anchorage groups compared with the two-bar anchorage groups.

- Demand on the column section was sufficient to produce one-way shear failure for the four bar anchorage group. Externally applied axial force increased the shear demand on the column due to the higher anchorage capacity. The shear capacity of the column increased at a higher rate than the demand from the anchorages with the externally applied axial column compression.

- Column sections with transverse reinforcement exhibited greater capacity than comparable specimens without transverse reinforcement. The ties were seen to increase capacity on average by 15%. Ties better constrained the concrete at failure, limiting the depth of penetration of the observed concrete wedge at pullout.

- The service level dead load axial force magnitude applied to the column increased the anchorage capacity of the specimens by 60% on average. Further increasing the axial force to the 1957 AASHO specified maximum allowable column stress did not significantly increase the anchorage capacity.

- The application of column axial compression force reduced the observed crack angles during pullout testing, when compared to otherwise similar specimens without applied axial compression. Specimens with the highest applied axial load exhibited the shallowest crack angle of 15° with respect to horizontal.

- The benefit of column axial compression stress acting transverse to the anchorage splitting plane is neglected by current US building and bridge design specifications. These design specifications underestimated the available anchorage strength more substantially for specimens with axial compression.

- A development length modification factor (κ) was introduced to include the beneficial effects of column axial compression stress acting transverse to the splitting plane. The addition of active confinement effects enabled better prediction of anchorage capacity for the specimens and may provide a better estimate of capacity for vintage 1950's RCDG flexural bar anchorages terminating in column sections.

- Upper and lower limits on κ, were established to restrict the benefit of high column compression stress due to limitations seen in previous research and neglect the contribution of low column axial compression stresses. The anchorage length modification factor κ is only applicable to anchorage conditions similar to those tested, and further research is needed to provide additional statistical measures of uncertainty over a broader range of member proportions, axial force magnitudes, and anchorage details.

- Additional research is needed to provide better statistical measures of the uncertainties over a broader array of member proportions, axial force ranges, and anchorage details.

4.0   REFERENCES

ACI Committee 208-58, "Test Procedure to Determine Relative Bond value of Reinforcing Bars," ACI Standards 1964, Michigan: American Concrete Institute, 1964.

ACI Committee 318, "Building Code Requirements for Structural Concrete," ACI 318-05 and Commentary ACI 318R-05, Michigan: American Concrete Institute, 2005.

ACI Committee 408R-03, Bond and Development of Straight Reinforcing Bars in Tension, ACI Manual of Concrete Practice Part 5, 2004, pp. 1-49.

American Association of State Highway Officials, "Standard Specifications For Highway Bridges," 1944, pp. 146-147.

American Association of State Highway Officials, "Standard Specifications For Highway Bridges," 1949, pp. 149-150, 190-191.

American Association of State Highway Officials, "Standard Specifications For Highway Bridges," 1953, pp. 182-183.

American Association of State Highway Officials, "Standard Specifications For Highway Bridges," 1957, pp. 36-37.

American Association of State Highway Officials, "Standard Specifications For Highway Bridges," 1961, pp. 39-40.

American Association of State Highway Officials, "Standard Specifications For Highway Bridges," 1969, pp. 55.

American Association of State Highway Officials, "Standard Specifications For Highway Bridges," 1973, pp. 57-58, 93.

American Association of State Highway and Transportation Officials, "Standard   Specifications For Highway Bridges," 1996, pp. 190-191.

American Association of State Highway and Transportation Officials, "Standard Specifications For Highway   Bridges," 1998, pp. 5-138, 5-141.

American Association of State Highway Officials, "Standard Specifications For Highway Bridges," 2004, pp. 5-136, 5-139.

ASTM A615/A615M-05a, "Standard Specification for Deformed and Plain Carbon-Steel Bars for Concrete Reinforcement," ASTM International, 2005, pp. 329-333.

ASTM A305-50T, "Minimum Requirements for the Deformations of Deformed Steel Bars for Concrete Reinforcement," ASTM International, 1950, pp. 218-220.

ASTM C 39/C 39M-05, "Standard Test Method for Compressive Strength of Cylindrical Concrete Specimens," ASTM International, 2005, pp. 21-27.

ASTM C 617-98, "Standard Practice for Capping Cylindrical Concrete Specimens," ASTM International, 2005, pp. 1-5.

ASTM E8-04, "Standard Test Methods for Tension Testing of Metallic Materials," ASTM International, 2005, pp. 64-87.

Baldwin, M.I., and Clark, L.A., "The Assessment of Reinforcing Bars with Inadequate Anchorage," *Magazine of Concrete Research*, V. 47, No. 171, June 1995, pp. 95-102.

Cairns, J., and Jones, K, J., "Bond Performance of Ribbed Reinforcing Bars in Lapped Joints," Bond in Concrete, Ed. Bartos, P., *Applied Science Publisher*, 1982, pp. 342-352.

Cairns, J., and Jones, K., "Influence of Rib Geometry on Strength of Lapped Joints: An Experimental and Analytical Study," *Magazine of Concrete Research*, V. 47, No. 172, Sept. 1995, pp. 253-262.

CEB-FIP Commission 3, "Practical Design Working Group on Recommendations for Practical Design of Structural Concrete," SETO, London, 1999.

Chapman, A. R., and Shah, S. P., "Early-Age Bond Strength in Reinforced Concrete," ACI Material Journals, V. 84, No. 6, Nov. 1987, pp. 501-509.

Clark, A. P., "Comparative Bond Efficiency of Deformed Concrete Reinforcing Bars," *Journal of the American Concrete Institute Proceedings*, V. 18, No. 4, Dec. 1946, pp. 381-   400.

Clark, A. P., "Bond of Concrete Reinforcing Bars" *Journal of the American Concrete Institute Proceedings*, V. 21, No. 3 Nov. 1949, pp. 161-184.

Darwin, D., McCabe, S,L. and Idun E,K., and Schoenekase, S, P., "Development Length Criteria: Bars Not Confined by Transverse Reinforcement," *ACI Structural Journal*, V. 89, No. 6, Nov.-Dec. 1992, pp. 709-720

Darwin, D., and Graham, E, K., "Effect of Deformation Height and Spacing on Bond Strength of Reinforcing Bars," *ACI Structural Journal*, V. 90, No. 6, Nov.-Dec. 1993, pp.646-   657.

Darwin, D., "Tension Development Length and Lap Splice Design for Reinforced Concrete Members," *Progress in Structural Engineering and Materials*, Vol. 7, No. 4, Oct-Dec 2005, pp. 210-225.

Darwin, D., and Lutz, A. L., and Zuo, J., "Recommended Provisions and Commentary on Development and Lap Splice Lengths for Deformed Reinforcing Bars in Tension," ACI Structural Journal, Vol. 102, No. 5, Nov.-Dec. 2005, pp. 892-900.

Doerr, K., "Bond Behavior of Ribbed Reinforcement under Transversal Pressure," *Nonlinear behavior of reinforced concrete structures; contributions to IASS symposium,* International Association for Shell Structures, V. 1, July 3-7, 1978, pp. 13-24.

Eligehausen, R., and Popov, E., and Bertero, V. V., 1983 "Local Bond Stress-Slip Relationships of Deformed Bars under Generalized Excitation," *UCB/EERC Report 83-82*, Earthquake Engineering Research Center, University of California at Berkeley, Berkeley, Calif.

Engstrom B., and Magnusson, J., and Huang, Z., "Pull-out Behavior of Ribbed Bars in Normal And High-Stress Concrete with Various Confinements," Bond and Development of Reinforcement, A Tribute to Dr. Peter Gergely, Ed. Leon, R., *ACI International*, SP-180, 1998, pp. 215-242.

Ezeldin, S. A., and Balaguru, P. N., "Bond Behavior of Normal and High Strength Fiber Reinforced Concrete," *ACI Material Journal*, V. 86, No. 5, Sept.- Oct. 1989, pp. 515-524.

Ferguson, P. M., and Turpin R. D., and Thompson N. J., "Minimum Bar Spacing as a Function of Bond and Shear Strength," *Journal of the American Concrete Institute Proceedings* V. 50, No. 10, June 1954, pp. 869-887.

Ferguson, P. M., and Breen, J. E., and Thompson N. J., "Pullout Tests on High Strength Reinforcing Bars," *Journal of the American Concrete Institute Proceedings*, V. 62, No. 8, Aug. 1965, pp. 933-949.

Ferguson, P.M., <u>Reinforced Concrete Fundamentals</u>, New York, John Wiley and Sons, 1979, pp.169-212.

Fujii, S., and Morita, S., "Bond Capacity of Deformed Bars Due to Splitting of Surrounding Concrete," Bond in Concrete, Ed. Bartos, P., *Applied Science Publisher*, 1982, pp.331-341.

Gambarova, G., and Karakoc, C., "Shear-Confinement Interaction at the Bar-to-Concrete Interface," Bond in Concrete, Ed. Bartos, P., *Applied Science Publisher*, 1982, pp. 82-96.

Gambarova, P. G. and Rosati, G., "Bond and splitting in reinforced concrete: test results on bar pull-out," *Materials and Structures*, V. 29, June 1996, pp.267-276.

Goto, Y., "Cracks Formed in Concrete Around Deformed Tension Bars," *ACI Journal Proceedings*, V.68, No. 4, April. 1971, pp. 244-251.

Harajli, H.; Hamad, B. S., and Rteil, A. A., "Effect of Confinement of Bond Strength between Steel Bars and Concrete," *ACI Structural Journal*, V. 101, No. 5, Sept.- Oct. 2004, pp. 595-603.

Higgins, C., and Farrow, W III, C., and Ptisuk, T., and Miller, T. H., and Yim, S. C., Holcomb, G. R., Cramer, S. D., Covino, B. S., Bullard, S. J., Ziomek-Moroz, M., and Matthes, S. A., "SPR 326 Shear Capacity Assessment of Corrosion-Damaged Reinforced Concrete Beams," Oregon Department of Transportation, Salem, OR, 2003, pp. 19.

Higgins, C., and Yim, S. C., and Miller, T. H., Robelo, M. J., and Potisuk, T., "SPR 341: Remaining Life of Reinforced Concrete Beams with Diagonal-Tension Cracks," Oregon Department of Transportation, Salem, OR, 2004.

Higgins, C., and Miller, T., and Rosowsky, D. V., and Yim, S. C., and Potisuk, T., Daniels, T. K., Nicholas, B. S., Robelo, M. J., and Lee, A., and Forrest, R. W., "SPR 350 Assessment Methodology for Diagonally Cracked Reinforced Concrete Deck Girder," Oregon Department of Transportation, Salem, OR, 2004.

Howell, D., and Higgins, C. "Bond and Development of Deformed Square Reinforcing Bars," *ACI Journal Proceedings*, In print.

Jeppsson, J., and Thelandersson, S., "Behavior of Reinforced Concrete Beams with Loss of Bond at Longitudinal Reinforcement," *Journal of Structural Engineering*, V. 129, No. 10, Oct. 2003, pp. 1376-1383.

Kong, F., and Teng, S., and Singh, A., and Tan, K., "Effect of Embedment Length of Tension Reinforcement on the Behavior of Lightweight Concrete Deep Beams," ACI Structural Journal, V. 93, No. 1, Jan.-Feb. 1996, pp.21-29.

Kuennen, T., "Taming Oregon's Cracked Bridges," *Better Roads*, Vol.76, No. 4, April 2006, pp. 54-64.

Large, G. E., <u>Basic Reinforced Concrete Design: Elastic and Creep</u>, New York: Ronald, 1957, pp. 22, 58.

Lutz, L. A., and Gergely, P., "Mechanics of Bond and Slip of Deformed Bars in Concrete," *ACI Journal Proceedings*, V.64, No.11, Nov. 1967, pp.711-721.

Lutz, A. L., "Information on the Bond of Deformed Bars from Special Pullout Tests," *ACI Journal Proceedings*, V. 67, No. 11, Nov. 1970, pp. 885-887.

MacGregor, G. J., and Wight, K. J., <u>Reinforced Concrete Mechanics and Design</u>, New Jersey, Prentice Hall, 2005, pp. 328-399.

Mains, R. M., "Measurement of the Distribution of Tensile and Bond Stresses Along Reinforcing Bars," *Journal of the American Concrete Institute*, Vol. 48, No. 3, Nov.   1951, pp. 225-252.

Malvar, J., "Bond of Reinforcement Under Controlled Confinement," *ACI Materials Journal*, V. 89, No. 6, Nov.-Dec. 1992, pp. 593-601.

Mo, Y.L., and Chan, J., "Bond and Slip of plain Rebar in Concrete," *Journal of Materials in Civil Engineering*, V. 8, No. 4, Nov. 1996, pp. 208-211.

Mylrea, T. D., "Bond and Anchorage," *Journal of the American Concrete Institute Proceedings*, Vol.44, No. 3, March 1948, pp. 521-552.

Nagatomo, K., and Kaku, T., "Confinement Stress Dependant Bond Behaviors under lateral compressive and tensile stress' Bond in Concrete," *International Conference on Bond in Concrete*, Riga Technical University, Oct. 17-19, 1992, pp. 1-69 - 1-78.

Navaratnarajah, V., and Speare, P. R. S., "An experimental study of the effects of lateral pressure on the transfer bond of reinforcing bars with variable cover," *Proceedings of the Institution of Civil Engineers*, V.81, No. 2, Dec. 1986, pp. 697-715.

ODOT, "Research, Development and Technology Transfer Program," Oregon Department of Transportation,<http://www.oregon.gov/ODOT/TD/TP_RES/docs/Reports/2006AnnualReport.p df>, Accessed Jan. 29, 2006.

ODOT, "Research, Development and Technology Transfer Program," Oregon Department of Transportation,<http://www.oregon.gov/ODOT/TD/TP_RES/docs/Reports/2005AnnualRe port.pdf>, Accessed Jan. 29, 2006.

ODOT, "Bridge Inventory and Database," Oregon State University, 2006.

Orangun, C. O., and Jirsa, J. O., and Breen, J. E., "The Strength of Anchored Bars: A Reevaluation of Test Data on Development Length and Splices," *Research Repot* No. 154-3F, Center for Highway Research, The University of Texas at Austin, Jan. 1975.

Orangun, C. O., and Jirsa, J. O., and Breen, J. E., "A Reevaluation of Test Data on Development Length and Splice," *ACI Journal Proceedings*, V. 74, No. 3, March 1977, pp. 114- 121.

Peabody, D. Jr., The Design of Reinforced Concrete Structures, New York: Wiley and Sons, 1946, pp. 45,

Reese C. R., "New Style Deformed Reinforcing Bars," *Journal of the American Concrete Institute Proceedings*¸ Vol.21, No. 9, May 1950, 681-688.

Robins, P. J., and Standish, I. G., "Effect of Lateral Pressure on Bond of Reinforcing Bars in Concrete," Bond in Concrete, Ed. Bartos, P., *Applied Science Publisher*, 1982, pp. 262-272.

Robins, P. J., and Standish, I. G., "The influence of lateral pressure upon anchorage bond," Bond in Concrete, *Magazine of Concrete Research*, V.36, No. 129, Dec. 1984, pp. 262-272.

Schroeder, H, P., and Wood, T, B., "Concrete/Reinforcing Steel Bond Strength of Low-Temperature Concrete," *Journal of Cold Regions Engineering*, V. 10 No. 2, June 1996, pp. 93-117.

Soroushian, P., and Choi, K. B., "Local Bond of Deformed Bars with Different Diameters in Confined Concrete," *ACI Structural Journal*, V. 86, No. 2, Mar.-Apr. 1986, pp. 217-222.

Soroushian, P., and Choi, K. B., "Analytical Evaluation of Straight Bar Anchorage Design in Exterior Joints," *ACI Structural Journal*, V. 88, No. 2, Mar.-Apr. 1991, pp. 161-168

Ueda, T.; Lin, I.; and Hawkins, N.M., "Beam Bar Anchorage in Exterior Column-Beam Connections," *ACI Journal*, V. 83, May-June 1986, pp. 412-422.

Untrauer, R. E., and Henry, R. L., "Influence of Normal Pressure on Bond Strength," *Journal Of the American Concrete Institute Proceedings*, V. 62, No. 5, May 1965, pp. 577-585.

Walker, P. R., and Batayneh, M. K., and Regean, P. E., "Bond strength tests on deformed reinforcement in normal weight concrete," *Materials and Structures*, V. 30, Aug.- Sept. 1997, pp. 424-429.

Walker, P. R., and Batayneh, M. K., and Regean, P. E., "Measured and design band strenghts of deformed bars, including the effect of later compression," *Materials and Structures*, V. 51, No. 1, Feb.1999 pp. 13-26.

APPENDIX A

Table 1A - Input Values for AASHTO and ACI 318-05.

Spec. Name	f'_c	f'_c	P	f_y	d_b	A_b	# of Bars	$l_{d\ exp}$	$f_y/\sqrt{(f'c)}$	Atr	fyt	b	d	a	jd	S	n	One-Half Center to Center Spacing	Center of Bar to Nearest Concrete Edge	Max. App. Force	Max. App. Avg. Force
	psi	ksi	Kips	in²	in	in²		in	psi	in²	(ksi)	in	in	in	in	in		in	in	kips	lbs
1M08	4145	4.145	0	66	1.41	1.56	1	8	1025	3.12	71	24	21.3	2.6	19.98	20.0	1	0	12	46.3	46300
1M012	4356	4.36	0	66	1.41	1.56	1	12	1000	3.12	71	24	21.3	2.5	20.05	20.0	1	0	12	86.0	86000
2L021	3550	3.55	0	66	1.41	1.56	2	21	1108	3.12	66	24	21.3	2.8	19.88	19.9	2	6	6	167.7	83850
2M021	3550	3.55	0	66	1.41	1.56	2	21	1108	3.12	66	24	21.3	2.8	19.88	19.9	2	6	6	200.2	100100
4L021	3786	3.79	0	66	1.41	1.56	4	21	1073	3.12	66	24	21.3	2.7	19.96	20.0	4	2	4	214.3	53575
4M021	3786	3.79	0	66	1.41	1.56	4	21	1073	3.12	66	24	21.3	2.7	19.96	20.0	4	2	4	236.2	59050
4L221	3100	3.10	200	66	1.41	1.56	4	21	1185	3.12	66	24	21.3	3.3	19.7	19.7	4	2	4	300.7	75175
4M221	3000	3.00	200	66	1.41	1.56	4	21	1205	3.12	66	24	21.3	3.4	19.6	19.6	4	2	4	338.5	84630
4L521	3200	3.20	500	66	1.41	1.56	4	21	1167	3.12	66	24	21.3	3.1	19.7	19.7	4	2	4	315.5	78873
4M521	3100	3.10	500	66	1.41	1.56	4	21	1185	3.12	66	24	21.3	3.3	19.7	19.7	4	2	4	180.38	90190

Table 2A: Physical and Material Properties Used for Analysis in ACI 318-05

Specimen	f'_c	p	f_y	Bar Φ	Bar Area	# of Bars	$L_{experimental}$ Length	$f_y/\sqrt{f'_c}$	One-Half Center to Center Spacing	Center of Bar to Nearest Concrete Edge	Maximum Applied Force	Ultimate Bar Stress
	psi	psi	ksi	in	in^2		in	psi	in	in	kips	ksi
4L221	3100	347	66	1.41	1.56	4	21	1185	2.0	6.0	300.7	48.2
4M221	3000	347	66	1.41	1.56	4	21	1205	2.0	6.0	338.5	54.3
4L521	3200	868	66	1.41	1.56	4	21	1167	2.0	6.0	315.5	50.6
4M521	3100	868	66	1.41	1.56	4	21	1185	2.0	6.0	180.4	57.8
EPB (83)	4495	725	76.9	1.00	0.79	1	5	1147	-	3.5	37	47.3
UH 65.1	3610	361	92	1.128	1.00	1	6	1531	-	3	33.7	33.7
UH 65.2	3610	722	92	1.128	1.00	1	6	1531	-	3	41.9	41.9
UH 65.3	3610	180	92	0.75	0.44	1	6	1531	-	3	22.2	50.4
UH 65.4	3610	902	92	0.75	0.44	1	6	1531	-	3	21.3	48.4
UH 65.8	4480	224	92	1.128	1.00	1	6	1375	-	3	33.8	33.8
UH 65.9	4730	474	92	1.128	1.00	1	6	1338	-	3	45.7	45.7
UH 65.10	5090	763	92	1.128	1.00	1	6	1290	-	3	44.8	44.8
UH 65.11	5090	1018	92	1.128	1.00	1	6	1290	-	3	52.0	52.0
UH 65.12	4730	1185	92	1.128	1.00	1	6	1338	-	3	59.3	59.3
UH 65.19	4730	237	92	0.75	0.44	1	6	1338	-	3	27.6	62.7
UH 65.20	4280	428	92	0.75	0.44	1	6	1406	-	3	25.6	58.2
UH 65.21	5090	763	92	0.75	0.44	1	6	1290	-	3	25.2	57.2
UH 65.22	4730	948	92	0.75	0.44	1	6	1338	-	3	33.4	75.8
UH 65.23	5090	1272	92	0.75	0.44	1	6	1290	-	3	33.2	75.5
UH 65.27	6410	320	92	1.128	1.00	1	6	1149	-	3	42.2	42.2
UH 65.28	5920	346	92	1.128	1.00	1	6	1196	-	3	35.8	35.8
UH 65.29	6460	970	92	1.128	1.00	1	6	1145	-	3	62.7	62.7
UH 65.30	6920	1383	92	1.128	1.00	1	6	1106	-	3	55.9	55.9
UH 65.31	6460	1938	92	1.128	1.00	1	6	1145	-	3	67.7	67.7
UH 65.34	6460	646	92	0.75	0.44	1	6	1145	-	3	34.8	79.2
RS (82)	4350	203	65.3	0.47	0.173	1	3.9	990	-	0.787	6.1	35.1
RS (82)	4350	290	65.3	0.47	0.173	1	3.9	990	-	0.787	6.7	39.0
RS (82)	4350	565.5	65.3	0.47	0.173	1	3.9	990	-	0.787	7.4	42.9
RS (82)	4350	754	65.3	0.47	0.173	1	3.9	990	-	0.787	8.0	46.1
RS (82)	4350	1218	65.3	0.47	0.173	1	3.9	990	-	0.787	9.6	55.2